Norwegian University Of Science and Technology
Faculty of Engineering and Technology

Institute for Energy Technology

University of Belgrade
Faculty of Mechanical Engineering

The long-term co-operative project

Master Degree Program:
Sustainable Energy and Environment in Serbia

Heat-Integrated Distillation Columns
-Analysis and Modelling-
with
Advanced Distillation
as Supporting Subject

M.Sc.- *candidate* Dimitrije R. Djordjevic

Trondheim, Norway

December 2003

Abstract

In this work, a distillation system with heat-integrated prefractionator columns is analysed. The equilibrium (theoretical) stage concept is used and constant relative volatility was assumed. Using short cut calculations three ternary mixtures, taken from literature, were considered. The most promising mixture is considered further. Using mathematical model self-optimisation study was done. According to the results from the self-optimisation study, a control structure was adopted, and further analysed. Dynamical performance of the system for different disturbances in feed composition and flow rate has been simulated.

Keywords. Heat-integrated columns, prefractionator arrangement, optimal operation, self-optimisation study, control structure simulation

Acknowledgement

I wish to thank Professor Truls Gundersen for his effort in finding me a project assignment. For guidance and help in my work I wish to thank my mentor in Norway Professor Sigurd Skogestad, mentor in Serbia Professor Jacimovic Branislav, PhD student Hilde Engelien and Dr Srbislav Genic.

Contents

Nomenclature

$x_{n,i}$ - Composition in liquid phase on tray ***n*** for component ***i***

$y_{n,i}$ - Composition in vapour phase on tray ***n*** for component ***i***

M_n - Amount of liquid on tray ***n***

F_n - Feed flow rate on tray ***n***

D - Distillate flow rate

B - Bottom product flow rate

$z_{n,i}$ - Composition of feed for ***n*** tray and ***i*** component

W_n - Side stream flow rate for tray ***n***

L_n - Liquid flow rate from tray ***n***

V_n - Vapour flow rate from tray ***n***

T - Temperature

p - Pressure

h_l - Enthalpy of liquid phase

h_v - Enthalpy of vapour phase

Δh_{sat} - Enthalpy of saturation

Q_n - Heat flux on tray ***n***

$w_{i,n}$ - Molar flow rate of component ***i*** above tray ***n***

r - Recovery factor

a_i - Relative volatility of component ***i***

f - Underwood root

t - Time

Introduction

Distillation is a very important industrial separation technology. It is commonly used for high purity separation since any degree of separation can be obtained with a fixed energy consumption by increasing the number of equilibrium stages. Distillation columns are used for about 95% of liquid separations and the energy use from this process is estimated as 3% of the world energy consumption [22]. With rising energy costs and growing environmental problems there is a need to reduce the energy use in industry. For the distillation process there are potentials for large energy savings by applying different methods of heat integration.

In this work, a heat-integrated distillation system with prefractionator was studied. This is a heat-integrated solution with big energy saving potentials. This arrangement can decrease energy consumption with more than 50%, as shown in the short cut calculations in this work.

Unfortunately, systems with heat-integrated prefractionator are very difficult to control. In this work self-optimisation study and dynamical analyse of was done. All analysis was done for a ternary mixture.

1. Basic Distillation Theory

1.1 Equilibrium Stage Concept

In this work, a distillation system with staged columns is analysed. It is established that calculations based on equilibrium stage concept (with the number of stages adjusted appropriately) fits data from most real columns very well [21]. The equilibrium (theoretical) stage concept is central in distillation. Figure 1.1 shows an equilibrium stage.

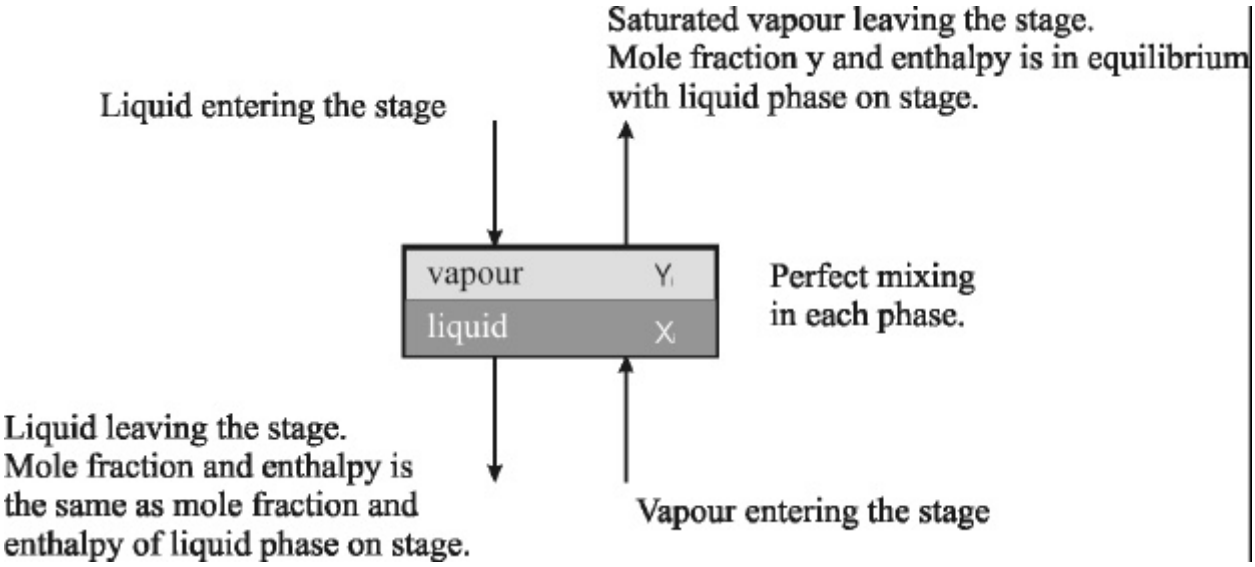

Figure 1.1. Equilibrium stage concept.

We assume vapour-liquid equilibrium on each stage, phases are ideally mixed. The stream, which leaves the stage, has the same composition and enthalpy as the liquid or vapour phase on the stage.

In many cases, we can assume constant relative volatility. In that case, equilibrium equations become:

$$y_{i,n} = \frac{a_i \cdot x_{i,n}}{\sum_{j}^{N_C} a_j \cdot x_{j,n}} \qquad a_i = const. \tag{1.1}$$

Where a_i is relative volatility, $x_{i,n}$ and $y_{i,n}$ are compositions of component ***i*** on stage ***n*** in the liquid and vapour phase. Relative volatility is:

$$a_i = \frac{y_i^* / x_i}{y_j^* / x_j} \tag{1.2}$$

In equation (1.2) the heaviest component is noted with index j, and with * equilibrium composition.

For a binary mixture with constant relative volatility the equilibrium curve is illustrated in Figure 1.2

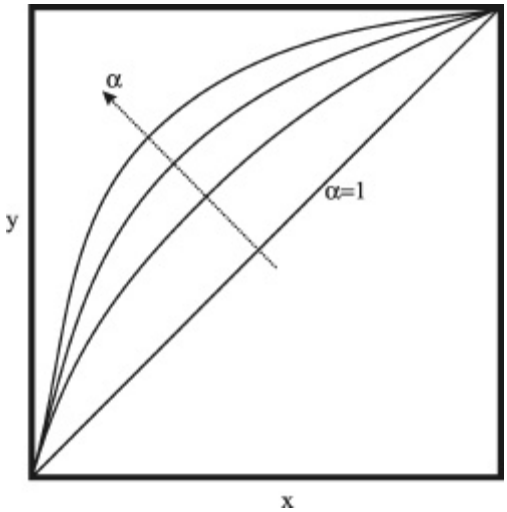

Figure 1.2. Equilibrium curve for ideal binary mixture.

Large relative volatilities imply large differences in boiling points and easy separation. Close boiling points imply relative volatilities closer to unity.

As recommended in literature [21], the temperature on a stage can be estimated as:

$$T = \sum \left(\frac{x_i + y_i}{2} \right) \cdot T_{bi} \tag{1.3}$$

In equation (1.3) T_{bi} is boiling temperature for pure component ***i.*** A suggested relationship between pressure and boiling temperature for a mixture considered is [21]:

$$p_{sat} = p_c \cdot \exp\left(\frac{A \cdot \left(1 - \frac{T_b}{T_c}\right) + B \cdot \left(1 - \frac{T_b}{T_c}\right)^{1,5} + C \cdot \left(1 - \frac{T_b}{T_c}\right)^{3,0} + D \cdot \left(1 - \frac{T_b}{T_c}\right)^{6,0}}{1 - \frac{T_b}{T_c}} \right) \tag{1.4}$$

Equations of equilibrium (1.1), (1.3) and (1.4) can be easily used for computer calculation.

1.2 Material Balance on a Distillation Stages

Based on the equilibrium stage concept, a distillation column section is modelled as shown in Figure 1.3. Note that we choose to number the stages starting from the bottom of the column. We assume perfect mixing in both phase inside a stage. The mole fraction of species ***i*** in the vapour leaving the stage with V_n is $y_{i,n}$, and the mole fraction in L_n is $x_{i,n}$.

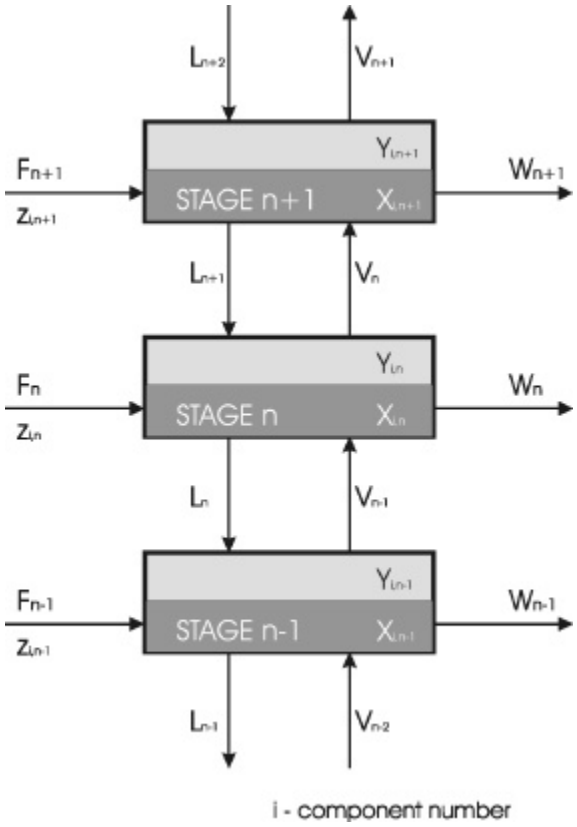

Figure 1.3 Staged distillation

On distillation stage ***n*** (see Figure 1.3) the mass balance equation for component ***i*** can be expressed as:

$$\frac{\partial\left(M_n \cdot x_{i,n}\right)}{\partial t} = F_n \cdot z_{i,n} - W_n \cdot x_{i,n} + V_{n-1} \cdot y_{i,n-1} - V_n \cdot y_{i,n} + \\ + L_{n+1} \cdot x_{i,n+1} - L_n \cdot x_{i,n} \tag{1.5}$$

Every stage can be additionally heated or cooled (heating flux is Q_n).
Energy balance for stage n is:

$$\frac{\partial\left(M_n \cdot h_n^l\right)}{\partial t} = h_{F,n} \cdot F_n - W_n \cdot h_n^l + V_{n-1} \cdot h_{n-1}^v - V_n \cdot h_n^v + L_{n+1} \cdot h_{n+1}^l - L_n \cdot h_n^l + Q_n \tag{1.6}$$

Summarized equations (1.5) for stage ***n*** and all components with respect to $\sum x_i = 1 \quad \sum y_i = 1$, gives the overall balance:

$$\frac{\partial(M_n)}{\partial t} = F_n - W_n + V_{n-1} - V_n + L_{n+1} - L_n \tag{1.7}$$

Usually we can assume constant vapour and liquid phase enthalpy:

$$\begin{aligned} h_l &= const. \\ h_v &= const. \end{aligned} \tag{1.8}$$

With these assumptions Equation (1.6) becomes:

$$h_l \cdot \frac{\partial(M_n)}{\partial t} = h_{F,n} \cdot F_n - W_n \cdot h_l + h_v \cdot (V_{n-1} - V_n) + h_l \cdot (L_{n+1} - L_n) + Q_n \tag{1.9}$$

Equations (1.5), (1.7) and (1.9) describe the dynamical behaviour of distillation columns. For steady state $\frac{\partial(....)}{\partial t} = 0$, so equations (1.5), (1.7) and (1.9) become:

$$0 = F_n \cdot z_{i,n} - W_n \cdot x_{i,n} + V_{n-1} \cdot y_{i,n-1} - V_n \cdot y_{i,n} + L_{n+1} \cdot x_{i,n+1} - L_n \cdot x_{i,n} \tag{1.10}$$

$$0 = h_{F,n} \cdot F_n - W_n \cdot h_l + h_v \cdot (V_{n-1} - V_n) + h_l \cdot (L_{n+1} - L_n) + Q_n \tag{1.11}$$

$$0 = F_n - W_n + V_{n-1} - V_n + L_{n+1} - L_n \tag{1.12}$$

Equations (1.11) and (1.12) can be rearranged into:

$$V_n = V_{n-1} + F_n \cdot (1 - q_n) + \hat{q}_n \tag{1.13}$$

$$L_{n+1} = L_n + W_n - q_n \cdot F_n + \hat{q}_n \tag{1.14}$$

In (1.13) and (1.14) $q_n = \frac{h_{v,sat} - h_{F,n}}{\Delta h_{sat}}$ and $\hat{q}_n = \frac{Q_n}{\Delta h_{sat}}$

Equations (1.10), (1.13) and (1.14) represent a closed system of equations and completely describe the steady state behaviours of distillation columns. But, since the equation of equilibrium (1.1) is higher degree then one, this system of equations can not be solved in a closed form. To get accurate solution from this system of equations it is necessary to use some numerical method.

1.3 Minimum Energy Usage – Infinite Number of Stages

Let us consider a simple column with one feed, and without side stream and additional heating, as shown on Figure 1.4.

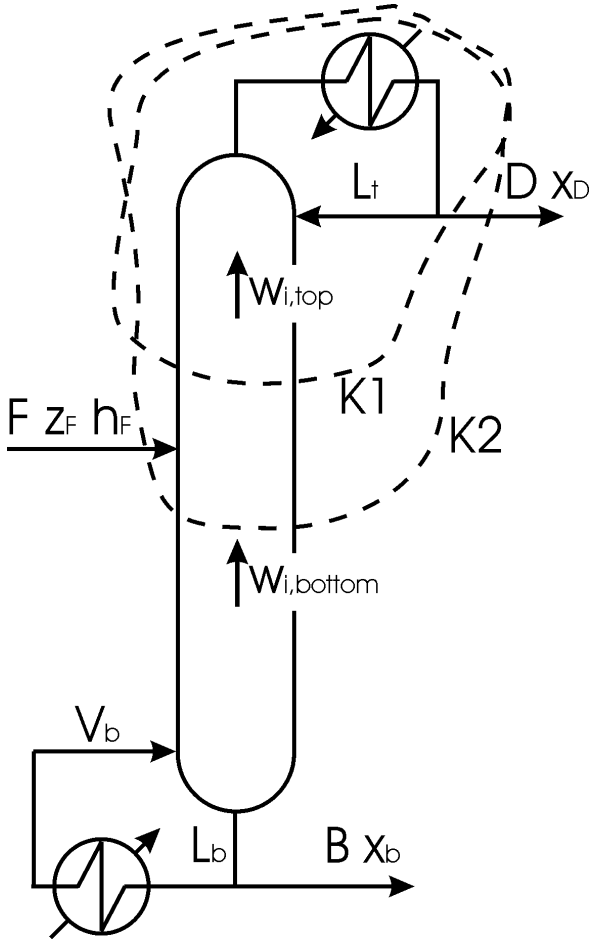

Figure 1.4. Simple distillation column

Equation (1.12) can be rearranged as:

$$\frac{1}{V}\cdot w_{i,n} = y_{i,n} - \frac{L}{V}\cdot x_{i,n+1} \tag{1.15}$$

where $w_{i,n}$ is the molar flow rate of component ***i*** above tray number ***n***.

For the top and bottom sections, $w_{i,n}$ can be calculated from the mass balance for the column:

$$w_{i,top} = D\cdot x_{i,D} \qquad \text{contour K1} \tag{1.16}$$

$$w_{i,bottom} = D\cdot x_{i,D} - F\cdot z_{F,i} = -B\cdot x_{i,B} \quad \text{contour K2} \tag{1.17}$$

Note that $w_{i,bottom}$ is negative, according to axes direction.

After multiplying Equation (1.15) with $\frac{a_i}{\sum_i a_i \cdot x_{i,n}}$ and summing for every component for each tray:

$$\frac{1}{V} \cdot \sum_i \frac{a_i \cdot w_{i,n}}{a_i - f} = \frac{\sum_i \frac{a_i^2 \cdot x_{i,n}}{a_i - f}}{\sum_i a_i \cdot x_{i,n}} - \frac{L}{V} \cdot \sum_i \frac{a_i \cdot x_{i,n+1}}{a_i - f} \tag{1.18}$$

Let left side in (1.18) to be equal to 1:

$$V = \sum_i \frac{a_i \cdot w_{i,n}}{a_i - f} \tag{1.19}$$

Equation (1.19) can be used to calculate f. The number of different solutions for f is the same as the number of components.

Substituting Equation (1.19) into Equation (1.18) gives:

$$\frac{f \cdot \sum_i \frac{a_i \cdot x_{i,n}}{a_i - f}}{\sum_i a_i \cdot x_{i,n}} = \frac{L}{V} \cdot \sum_i \frac{a_i \cdot x_{i,n+1}}{a_i - f} \tag{1.20}$$

Equations (1.20) and (1.19) are known as Underwood's equations and f as the Underwood's roots [1].
Equation (1.20) can be written for each tray and it is valid for any of the Underwood roots, so if we assume constant molar flow and divide one equation with root f_k with equation for root f_j, we have the following expression:

$$\frac{\sum_i \frac{a_i \cdot x_{i,n+1}}{a_i - f_k}}{\sum_i \frac{a_i \cdot x_{i,n+1}}{a_i - f_j}} = \left(\frac{f_k}{f_j}\right) \cdot \frac{\sum_i \frac{a_i \cdot x_{i,n}}{a_i - f_k}}{\sum_i \frac{a_i \cdot x_{i,n}}{a_i - f_j}} \tag{1.21}$$

From equation (1.21) the following equation can be developed:

$$\frac{\sum_i \frac{a_i \cdot x_{i,n+m}}{a_i - f_k}}{\sum_i \frac{a_i \cdot x_{i,n+m}}{a_i - f_j}} = \left(\frac{f_k}{f_j}\right)^m \cdot \frac{\sum_i \frac{a_i \cdot x_{i,n}}{a_i - f_k}}{\sum_i \frac{a_i \cdot x_{i,n}}{a_i - f_j}} \tag{1.22}$$

Equation (1.22) is only valid for trays with constant molar flows. This equation can be used to calculate the number of stages.

Underwood showed that in the top section (with ***Nc*** component) the roots (f) obey:

$$a_1 > f_1 > a_2 > f_2 > ... > a_{Nc} > f_{Nc}, \tag{1.23}$$

and for bottom section:

$$y_1 > a_1 > y_2 > a_2 > ... > y_{Nc} > a_{Nc} \tag{1.24}$$

In (1.24) with y is denoted Underwood's root in bottom section as with f in top section.

For theoretically infinite number of stages we have minimum flow rate trough the column. In that case, we have:

$$V \to V_{\min} \quad \Rightarrow \quad f_i \to y_{i+1} \tag{1.25}$$

Equation (1.19) for top and bottom section is:

$$V_T = \sum_i \frac{a_i \cdot w_{i,n}}{a_i - f_j} \tag{1.26}$$

$$V_B = \sum_i \frac{a_i \cdot w_{i,n}}{a_i - y_j} \tag{1.27}$$

Energy and mass balance for column in Figure 1.4 gives:

$$(1-q)\cdot F = V_T - V_B = \sum_i \frac{a_i \cdot w_{i,top}}{a_i - f_j} - \sum_i \frac{a_i \cdot w_{i,bottom}}{a_i - y_j} \tag{1.28}$$

In case of infinite number of stages and minimum vapour flow rate we may write:

$$V \to V_{\min} \quad \Rightarrow \quad f_i \to y_{i+1} \quad q_i \equiv f_i = y_{i+1} \tag{1.29}$$

In expression (1.29) q is the common root. If we use common roots in (1.28):

$$(1-q)\cdot F = \sum_i \frac{a_i \cdot \left(w_{i,top} - w_{i,bottom}\right)}{a_i - q_j} = \sum_i \frac{a_i \cdot z_{F,i}}{a_i - q_j} \cdot F \tag{1.30}$$

If we divided left and right side of (1.30) with ***F*** we obtain what is called the feed equation:

$$(1-q) = \sum_i \frac{a_i \cdot z_{F,i}}{a_i - q_j} \tag{1.31}$$

Equation (1.31) is only valid for minimum vapour flow rate (infinite number of stages). Using equation (1.31) we can find the common Underwood roots. Equation (1.27) can then be used to calculate the minimum vapour flow rate for different recovery fraction.

For a mixture with three components the minimum vapour flow rates in top section and bottom section are:

$$V_{top,\min} = \sum_{i=1}^{3} \frac{a_i \cdot w_{i,top}}{a_i - q_j} = \sum_{i=1}^{3} \frac{a_i \cdot r_{i,D} \cdot z_{F,i}}{a_i - q_j} \cdot F \tag{1.32}$$

$$V_{bottom,\min} = \sum_{i=1}^{3} \frac{a_i \cdot w_{i,bottom}}{a_i - q_j} = \sum_{i=1}^{3} \frac{-a_i \cdot r_{i,B} \cdot z_{F,i}}{a_i - q_j} \cdot F \tag{1.33}$$

For sharp AB/BC separation, which means that we do not have any light component in the bottom product and heavy component in the top product, we heave:

$$r_{A,D} = 1 \quad r_{B,D} = 0...1 \quad r_{C,D} = 0 \tag{1.34}$$

$$r_{A,B} = 0 \quad r_{B,B} = 0...1 \quad r_{C,B} = 1 \tag{1.35}$$

Substituting for the recoveries Equations (1.32) and (1.33) then become:

$$\frac{V_{top,\min}}{F} = \frac{a_A \cdot z_{F,A}}{a_A - q_j} + \frac{a_B \cdot r_{B,D} \cdot z_{F,B}}{a_B - q_j} \tag{1.36}$$

$$\frac{V_{bottom,\min}}{F} = -\frac{a_B \cdot r_{B,B} \cdot z_{F,B}}{a_B - q_j} - \frac{a_C \cdot z_{F,C}}{a_C - q_j} \tag{1.37}$$

The distillate flow rate can be expressed as function of recovery fraction:

$$\frac{D}{F} = \sum_i r_{i,D} \cdot z_{F,i} \tag{1.38}$$

For sharp separation AB/BC (1.38) is equivalent to:

$$\frac{D}{F} = z_{F,A} + r_{B,D} \cdot z_{F,B} \tag{1.39}$$

$$\frac{D}{F} = z_{F,A} + z_{F,B} \cdot \left(1 - r_{B,B}\right) \tag{1.40}$$

Using equations (1.39) and (1.40) in equations (1.36) and (1.37) leads to:

$$\frac{V_{top,\min}}{F} = \frac{a_A \cdot z_{F,A}}{a_A - q_j} + \frac{a_B}{a_B - q_j} \cdot \left(\frac{D}{F} - z_{F,A}\right) \tag{1.40}$$

$$\frac{V_{bottom,\min}}{F} = -\frac{a_C \cdot z_{F,C}}{a_C - q_j} + \frac{a_B}{a_B - q_j} \cdot \left(\frac{D}{F} - z_{F,A} - z_{F,B} \right) \tag{1.41}$$

Minimum vapour flow trough the column is:

$$\frac{V_{\min}}{F} = \max\left(\frac{V_{top,\min}}{F}, \frac{V_{bottom,\min}}{F} \right) \tag{1.42}$$

In case of a binary mixture, the minimum flow rate can be calculated using King's formula [21], here given for liquid feed (q=1):

$$L_{top,\min} = \frac{r_{L,D} - a \cdot r_{H,D}}{a - 1} \cdot F \tag{1.43}$$

$$V_{bottom,\min} = \frac{r_{H,B} - a \cdot r_{L,B}}{a - 1} \cdot F \tag{1.44}$$

King's formula can be developed from Underwood's equations (1.26), (1.27) and (1.31). For sharp separations and binary mixtures we get:

$$V_{B\min} = \frac{1}{a - 1} \cdot F + D \quad \text{(q=1)} \tag{1.45}$$

All equations shown above can be represented in $\frac{D}{F}$ - $\frac{V_{\min}}{F}$, so called as $V_{\min}$ diagram [21].
In $V_{\min}$ diagram equations (1.40) and (1.42) are lines and with respect to expression (1.42) we get line as shown on Figure 1.6, line between points $P_{AB} - P_{AC} - P_{BC}$. All other lines on Figure (1.5) are obtained in the same way. On Figure (1.5) are shown regions with different type of separations. On line $P_{AB} - P_{AC} - P_{BC}$ we have sharp separation AB/BC with minimum energy consumption. At point P_{AB} we have sharp separation A/BC and at point P_{BC} sharp separation AB/C, both with minimum energy consumption. Above this point, as shown with dashed lines we still have proper sharp separation, but with more energy consumption than the minimum.
Point P_{AC} is called the "preferred" sharp AB/BC separation. In that point, energy used for sharp separation AB/BC is at a minimum. Recovery factor in P_{AC} can be calculated from equation:

$$\frac{a_A \cdot z_{F,A}}{a_A - q_j} + \frac{a_B \cdot r_{B,D} \cdot z_{F,B}}{a_B - q_j} = \frac{a_A \cdot z_{F,A}}{a_A - q_k} + \frac{a_B \cdot r_{B,D} \cdot z_{F,B}}{a_B - q_k} \tag{1.46}$$

Equation (1.46) is developed from equations (1.42) using two different common roots, now recovery factor in P_{AC} is:

$$r_{B,D} = -\frac{a_A \cdot z_{F,A} \cdot (a_B - q_k) \cdot (a_B - q_j)}{a_B \cdot z_{F,B} \cdot (a_A - q_k) \cdot (a_A - q_j)} \tag{1.47}$$

Vapour flow rate can be calculated with equations (1.36) and (1.37) for a specific recovery.

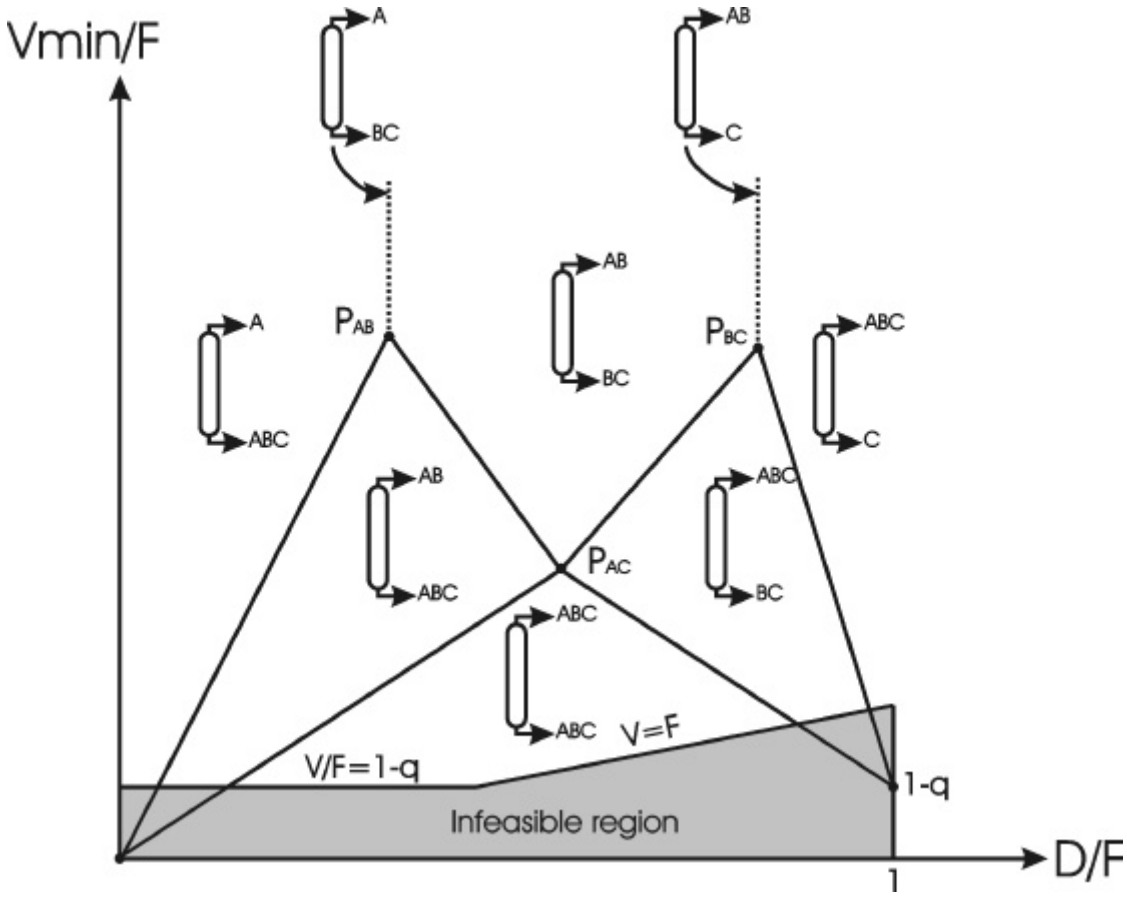

Figure 1.6. Regions of distributing feed component as function of (D/F) and (V/F)

Line (0,0)- P_{AB} represents separation A/ABC. Line P_{BC} -(1,1-q) represent separation ABC/C. Lines (0,0)- P_{AC} and P_{AC} -(1,1-q) represent separations AB/ABC and ABC/BC.

2. Model Description

Steady state behaviour of columns is described with equations (1.10), (1.13) and (1.14). These equations are not linear, and that can be a problem for calculations. However, for solving these equations, numerical methods are very good. MatLab has a tool ***fsolve*** for solving system of linear and non-linear matrix equations. ***Fsolve*** uses an iterative method known as the Gauss – Newton method. For using this tool, all equations have to be written as:

$$F(X)=0 \tag{2.1}$$

In equation (2.1) ***X*** is a matrix variable, and function is a matrix function. In addition, it is necessary to define the Jacobian of function ***F***. If we have ***Nt*** trays and a mixture with ***Nc*** components, then for one column matrix ***X*** can be the liquid composition on each tray. The dimension of the matrix in that case will be [Nc, Nt+2]. Two additional members are reserved for vapour and liquid composition, which are coming in column on top and bottom. For one tray, with steady state operation, the mass balance equation will be:

$$f_{i,n}=G_{n-1}\cdot y_{i,n-1}-G_n\cdot y_{i,n}+L_{n+1}\cdot x_{i,n+1}-L_n\cdot x_{i,n}+F_n\cdot z_{i,n}-W_n\cdot x_{i,n} \tag{2.2}$$

Function $f_{i,n}$ is member in matrix $F(X)$, ***i*** is component number and ***n*** is tray number. Jacobian of matrix $F(X)$ is calculated as partial derivative of all $f_{i,n}$ members with respect to all variables in matrix X. Jacobian is matrix J with dimension $\left(Nt+2, Nc\cdot\left(Nt+2\right)\right)$. Members of matrix J can be calculated as:

$$\frac{\partial f_{i,n}}{\partial x_{k,m}}=\frac{\partial f_{i,n}}{\partial y_{i,n}}\cdot\frac{\partial y_{i,n}}{\partial x_{k,m}}+\frac{\partial f_{i,n}}{\partial y_{i,n-1}}\cdot\frac{\partial y_{i,n-1}}{\partial x_{k,m}}+\frac{\partial f_{i,n}}{\partial x_{k,m}} \tag{2.3}$$

The composition in the vapour phase is a function of the compositions in liquid phase, and this function, for equilibrium assumption, is given by (1.1).

An other way to solve steady the state equations are to use equations for the dynamical model, and simulate long enough, until steady state operation is reached.

Dynamical behaviour is described by a system of differential equations. It is higher rank of equations then one, and it depends on the number of components. Only in case of one component, systems of differential equations become to be linear. Order of equations is one (first order system). This system of equations for three component mixture is impossible to be solved in closed form, but with numerical calculation, we can get solutions very close to correct ones. To solve sets of equations given by (1.5), (1.7) and (1.9) we may use some hybrid method.

In all numerical methods, time derivate is discretised. Let consider simple equation:

$$\frac{\partial f\left(x,y,t\right)}{\partial t}=g\left(f,x,y\right) \tag{2.4}$$

Where ***f*** is an unknown function and ***g*** is a known function. If we want to solve equation (2.4) with some numerical method we should first discretised left side in the equation (2.4):

$$\frac{\partial f(x,y,t)}{\partial t} \approx \frac{f(x,y,t+\Delta t)-f(x,y,t)}{\Delta t} \tag{2.5}$$

Right side in the equation (2.4) is known function and basic problem in numerical solution is should we use ***f*** on the right side in the equation (2.4) in future moment or past moment. However, we may use both in future moment and past moment as:

$$\frac{f(x,y,t+\Delta t)-f(x,y,t)}{\Delta t} = b\cdot g(x,y,t+\Delta t)+(1-b)\cdot g(x,y,t) \tag{2.6}$$

In the equation (2.6) b is a number between 0 and 1. In Figure (2.7) this problem is represented graphically. Black points are variables in the past time step, and red points are variables in the future time step. With arrows is represented, which variables we need to calculate a unknown variable ***A***. If b in the equation (2.6) is equal to 0 then variable ***A*** depends only on variables in past time steep, blue arrows Figure 1.7 a). If b in the equation (2.6) is equal to 1 then variable ***A*** depends only on variables in future time steep, green arrows Figure 1.7 b) . If b is between 0 and 1 then variable ***A*** depends on variables in the past time step and future time step Figure 1.7 c).

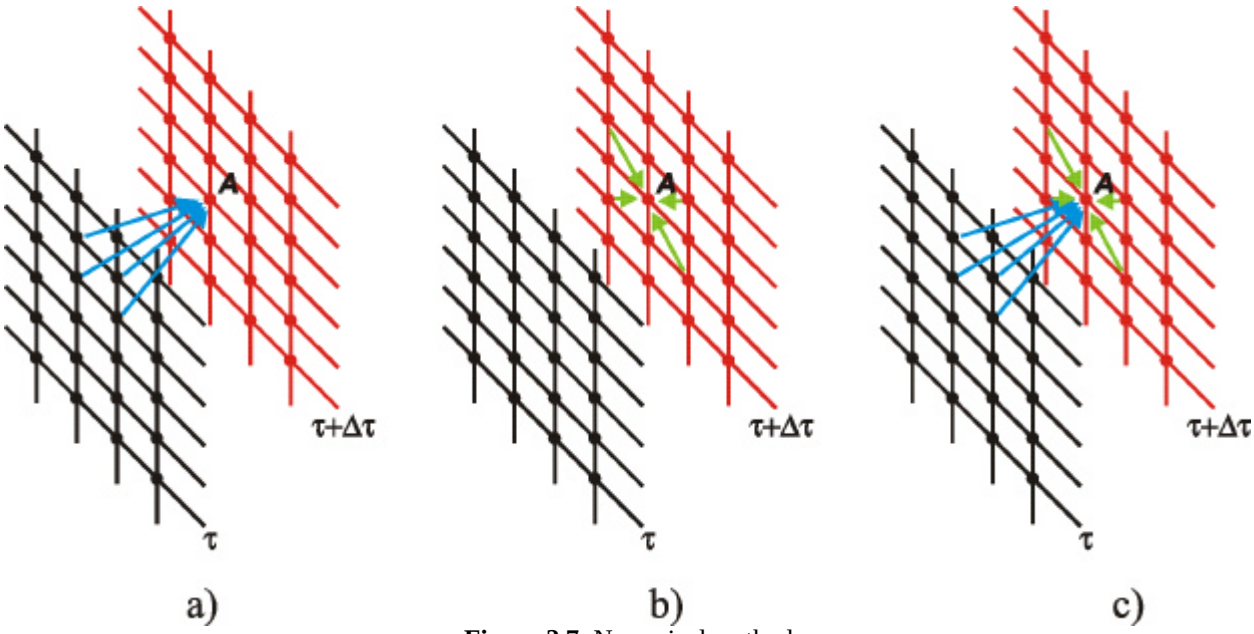

Figure 2.7. Numerical method

Equations (1.5) and (1.9), now can be written as:

$$\begin{aligned} & b\cdot\left(F_n - W_n + V_{n-1} - V_n + L_{n+1} - L_n\right)_{t=t_o+\Delta t} + \\ & +\left(1-b\right)\cdot\left(F_n - W_n + V_{n-1} - V_n + L_{n+1} - L_n\right)_{t=t_o} = \\ & = \frac{\left(M_n\right)_{t=t_o+\Delta t} - \left(M_n\right)_{t=t_o}}{\Delta t} \end{aligned} \tag{2.7}$$

$$\begin{aligned} & b\cdot(F_n\cdot z_{i,n} - W_n\cdot x_{i,n} + V_{n-1}\cdot y_{i,n-1} - V_n\cdot y_{i,n} + L_{n+1}\cdot x_{i,n+1} - L_n\cdot x_{i,n})_{t=t_0+\Delta t} + \\ & (1-b)\cdot(F_n\cdot z_{i,n} - W_n\cdot x_{i,n} + V_{n-1}\cdot y_{i,n-1} - V_n\cdot y_{i,n} + L_{n+1}\cdot x_{i,n+1} - L_n\cdot x_{i,n})_{t=t_0} = \\ & = \frac{\left(M_n\cdot x_{i,n}\right)_{t=t_0+\Delta t} - \left(M_n\cdot x_{i,n}\right)_{t=t_0}}{\Delta t} \end{aligned} \tag{2.8}$$

In Equations (2.7) and (2.8) the value b describes which method is used. Term b are variables in future time step and they are not known in each calculation. Term $\left(1-b\right)$ are variables in past time step and they are known in each calculation. If $b=0$ then we have *back in time method.* In that case we calculate new compositions and flow rates only considering variables in past time step. If $b=1$ then we have *forward in time method.* If $0<b<1$ then we have hybrid method, where the case $b=0{,}5$ is known as Crank – Nicholson method or scheme, which is used in these simulations.

Equations (2.7) and (2.8) are not linear equations, non-linear terms in those equations are: vapour compositions, and amount of liquid on trays. These terms can be linearised using Tailor's expansion (or polynomial).

If we develop vapour composition using Tailor's expansion, we get:

$$y_i = y_i^* + \sum_{j=1}^{N_C}\left(\frac{\partial y_i}{\partial x_j}\right)^*\cdot\left(x_j - x_j^*\right) + \frac{1}{2!}\sum_{j=1}^{N_C}\left(\frac{\partial^2 y_i}{\partial {x_j}^2}\right)^*\cdot\left(x_j - x_j^*\right)^2 + \ldots \tag{2.9}$$

In equation (2.9) (*****) denotes variables in past time step, other variables are in future next time step. Members after second member on left side in (2.9) can be neglected, and then we have linear equation instead equation (2.9). That linear equation can be written as:

$$y_i = y_i^* + \sum_{j=1}^{N_C}\left(d_{ij}\cdot\frac{y_i^*}{x_i^*} - \frac{y_i^*\cdot y_j^*}{x_j^*}\right)\cdot\left(x_j - x_j^*\right) \tag{2.10}$$

Liquid flow rate can be calculated using Francis' Weir formula. If amount of liquid on tray is ***M***, then liquid flow rate is:

$$L = k\cdot\left(M - M_w\right)^m \tag{2.11}$$

where M_w is the amount of liquid under the tray weir, and it is assumed constant. Coefficients ***k*** and ***m*** are also constant. From equation (2.11) we can develop:

$$M = M_w + \frac{L^{1/m}}{k} \tag{2.12}$$

Now the amount of liquid on each tray can be expressed using Tailor's polynomial:

$$M_n = M_n^* + \left(\frac{\partial M_n}{\partial L_n}\right)^* \cdot (L_n - L_n^*) + \frac{1}{2!} \cdot \left(\frac{\partial M_n}{\partial L_n}\right) \cdot \left(L_n - L_n^*\right)^2 + \ldots \tag{2.13}$$

As in equation (2.9) the terms after the second member on the left side of (2.13) can be neglected, giving linear equation instead of equation (2.13):

$$M_n = M_n^* + \frac{\left(L_n^*\right)^{\frac{1-m}{m}}}{m \cdot k} \cdot (L_n - L_n^*) \tag{2.14}$$

Using (2.10) and (2.14) equations (2.7) and (2.8) become linear equations, which can be easily solved.

For steady state calculation, we may use the same model as for dynamical calculations. In that case we can separately calculate flow rates, and keep them constant, for amount of liquid on tray we may use some constant number. It does not have to be correct amount of liquid on tray. In that case, we do not have to use equation (2.8). Equation (2.7) can be solved, as we solved the dynamical model. The end of iterations is when in two following iterations difference in compositions is small enough.

3. Introduction to Heat-Integrated Distillation System with Prefractionator

For ternary separations there are three classical separations schemes: direct split, indirect split and the prefractionator arrangement. In the Figures 3.1, 3.2 and 3.3,below all three schemes are shown.

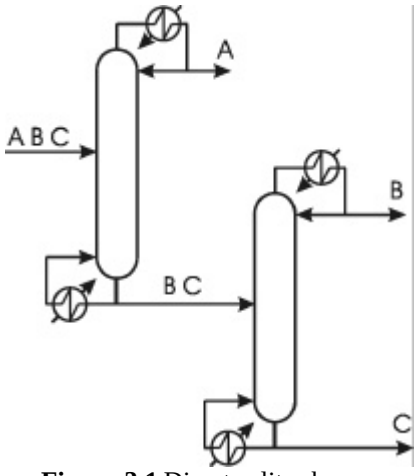

Figure 3.1 Direct split scheme

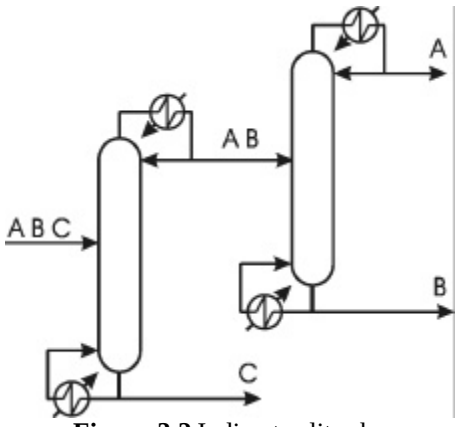

Figure 3.2 Indirect split scheme

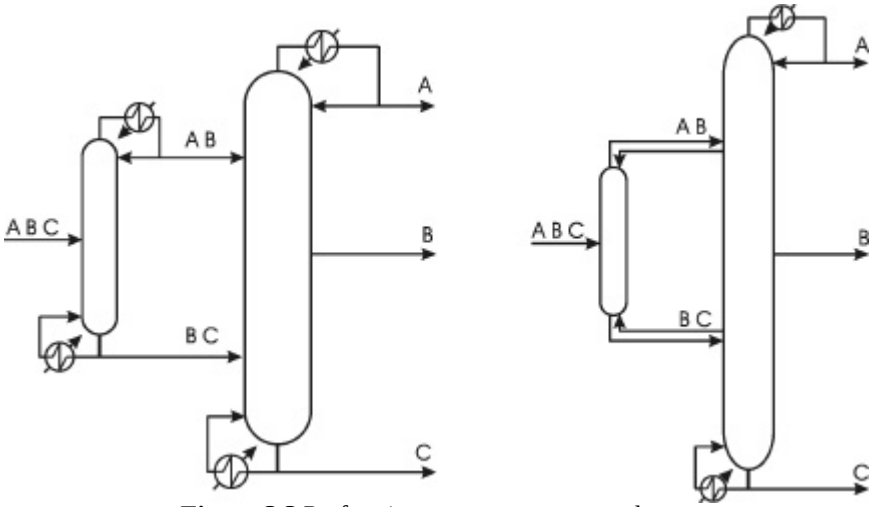

Figure 3.3 Prefractionator arrangement scheme

In all three schemes multi-effect heat integration is possible. The columns are integrated by combining the condenser of one column with the reboiler of another column. In that case, columns have to work on different pressures to keep sufficient temperature difference for heat transport. In literature, many works are published with subject which arrangement is the best one [12,13,14,15,17,18,21]. For saving energy heat integrated prefractionator arrangement has the best possibility. According to literature data [12,13], it is possible to save up to 70% of energy using heat integrated prefractionator arrangement.
Columns can be integrated forward or backward. In case of forward integration, the first column is run at a higher pressure than the second column. For the backward integration, the second column is run at a higher pressure than the first column.

In this work the forward integrated prefractionator arrangement is studied. Figure 3.4 below shows a simplified scheme for this arrangement.

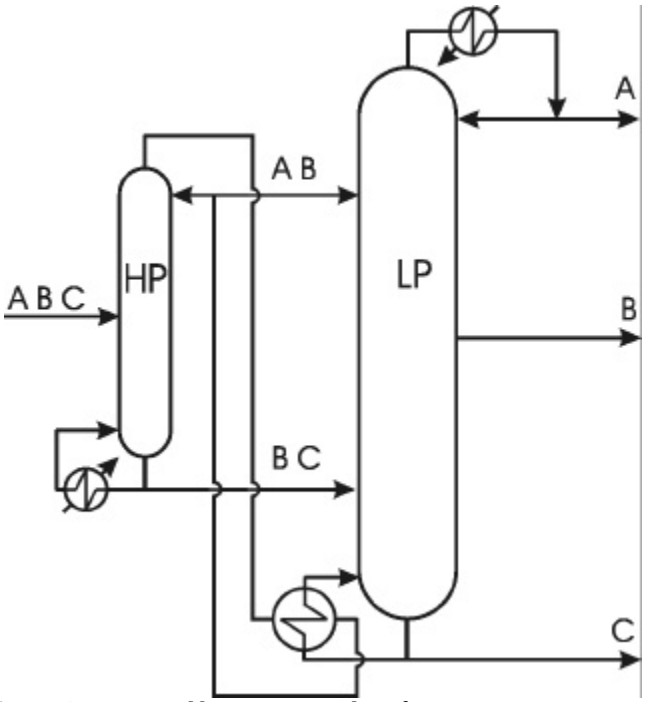

Figure 3.4 Forward heat integrated prefractionator arrangement

The condenser for the first column and the evaporator for the second column is combined in the same heat exchanger. In this work the possible energy saving, optimum operation and "self-optimisation" control and dynamical behaviours was studied for this system.

4. Introduction to Self-Optimising Control

The method of self-optimising control involves a search for the variables that, when kept constant, indirectly lead to near-optimal operation with acceptable loss. The procedure consists of six steps:

1) a degree of freedom (DOF) analysis,
2) definition of cost function,
3) identification of the most important disturbances,
4) optimisation,
5) identification of candidate controlled variables and
6) evaluation of loss with constant set point.

For the two-column scheme as shown in Figure 3.3 (left figure), there are seven degrees of freedom in steady state work. For the first column, there are three degrees of freedom. Those are the reflux ratio, distillate flow ratio and the pressure. For the second column, there are four degrees of freedom, the reflux ratio, the distillate, the pressure and duty of condenser.
If the two columns are heat integrated, as in Figure 3.4, the vapour flow in the second column depends on the vapour flow in first column, so we have one degree of freedom less than in two non-integrated columns. In this work feed mixtures with high purity products (99% mole fraction) are considered. In that case flow rate of final products are almost constant and approximately:

$$D_{p,i} = F \cdot z_{F,i} \tag{4.1}$$

According to equation (4.1) in second column we have two degrees of freedom less. Finally we have 7 – 3 = ***4*** degrees of freedom for heat integrated prefractionator arrangement with high purity products (99%). In this work for optimal operation analysis independent variables are: the pressure in first column and the pressure in second column; the reflux ratio in first column and the distillate flow rate between two columns.

The objective function for this system can be expressed as:

$$J = p_D \cdot D + p_S \cdot S + p_B \cdot B - p_F \cdot F - p_V \cdot V \tag{4.2}$$

The prices for final (p_D, p_S, p_B) products are constant, according to high purity. Price for feed is, also constant. Then equation (4.2) can be written as:

$$J = Const - p_V \cdot V \tag{4.3}$$

Optimal operation is when the objective function is at maximum, and then the profit is at maximum. If we chose constant pressure of heating steam, which we can if the pressure in the first column is constant, then maximum of the objective function ***J*** will be when the vapour flow trough first column is minimum.
The optimisation problem can then be formulated as finding minimum vapour flow rate for the first column, but at the same time, achieving a purity of products equal to or higher than 99% (the system constrains).

According to theory from chapter 1, we can consider heat-integrated columns in case of infinite number of trays, using D/F – Vmin/F diagram. If we have a system of two columns, as shown in Figure 3.5 below, we may draw D/F – Vmin/F diagrams for both columns in one figure.

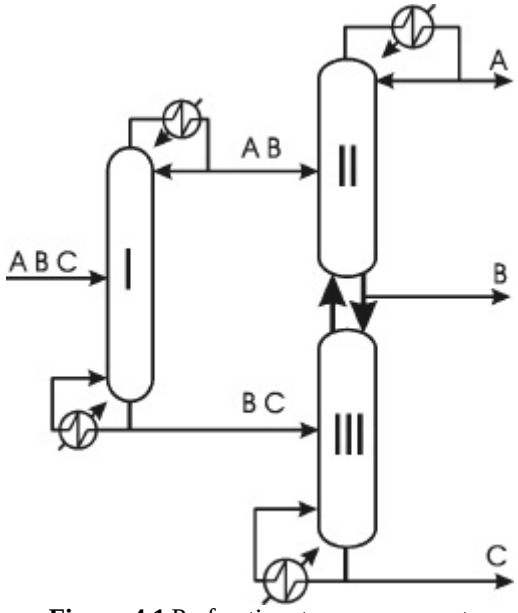

Figure 4.1 Prefractionator arrangement

The second column in Figure 4.1 above is split into two column sections (column II and III). Between section II and III we take medium component product. This scheme is equivalent to the scheme shown in Figure 3.3, but is clearer for considering. In column II we have sharp separation of A/B and in column III we have sharp separation of B/C. In the first column, column I, we have sharp separation between A and C. We can calculate the minimum flow rate in sections II and III as function of distillate flow rate from column I ($\frac{D_I}{F}$). In the second column (sections II and III) we will use equations for binary mixtures. Figure 4.2 below shows Vmin diagram for the system in Figure 4.1. The dot line represents minimum flow rate for column III, and pointed line represents minimum flow rate for column II. The solid line is for column I, this line is described on Figure 1.6. Possible working order for this sharp separation concept is:

$$z_{F,A} \leq \frac{D_I}{F} \leq z_{F,A} + z_{F,B} \tag{4.4}$$

Figure 3.6 can be used to easily establish the minimum energy consumption for the system with not-integrated columns:

$$Q_{\min} = \Delta H_{vap.} \cdot \min\left\{\left(V_{\min}\right)_I + \max\left\{\left(V_{\min}\right)_{II}, \left(V_{\min}\right)_{III}\right\}\right\} \tag{4.5}$$

This method can be used and for integrated columns, then (4.5) becomes:

$$Q_{\min} = \Delta H_{vap.} \cdot \min\left\{\max\left\{\left(V_{\min}\right)_{II}, \left(V_{\min}\right)_{III}, \left(V_{\min}\right)_{I}\right\}\right\} \tag{4.6}$$

In equations (4.5) and (4.6) vapour flow rate is function of $\frac{D_I}{F}$. Diagram represented in Figure 4.2 is for infinite number of stages.

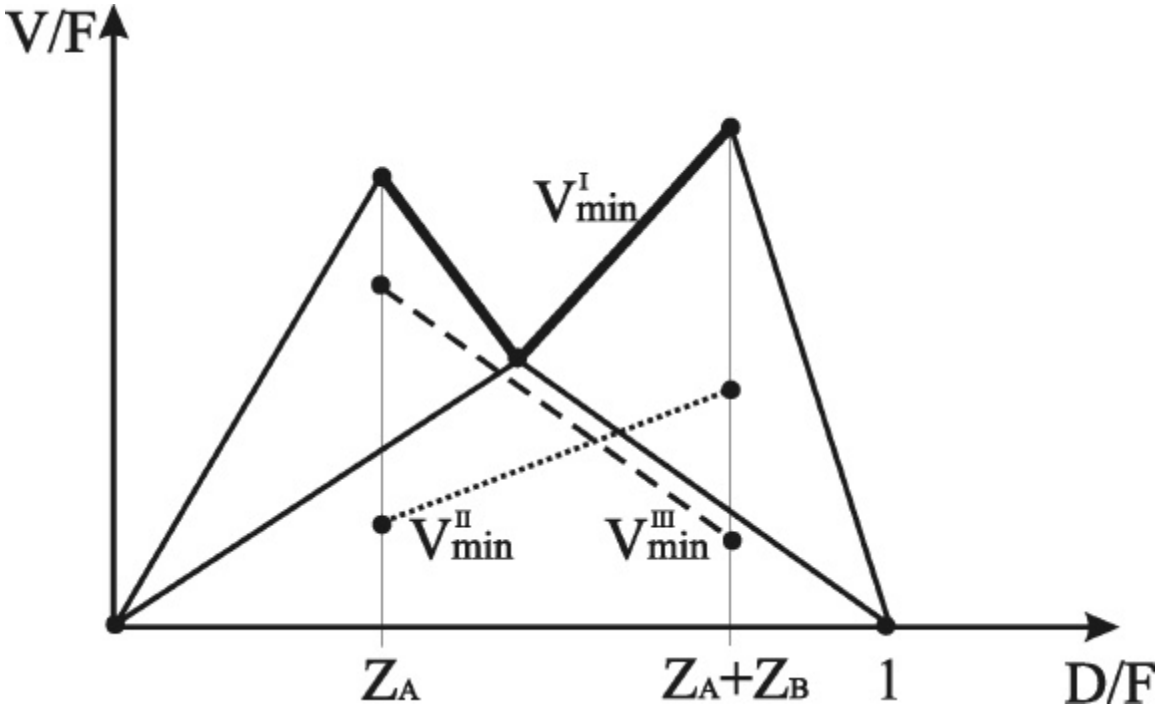

Figure 4.2 D/F – V/F diagram system with prefractionator

Figure 4.3, on the next page, shows how we can calculated minimum flow rate for integrated columns using D/F – V/F diagram.

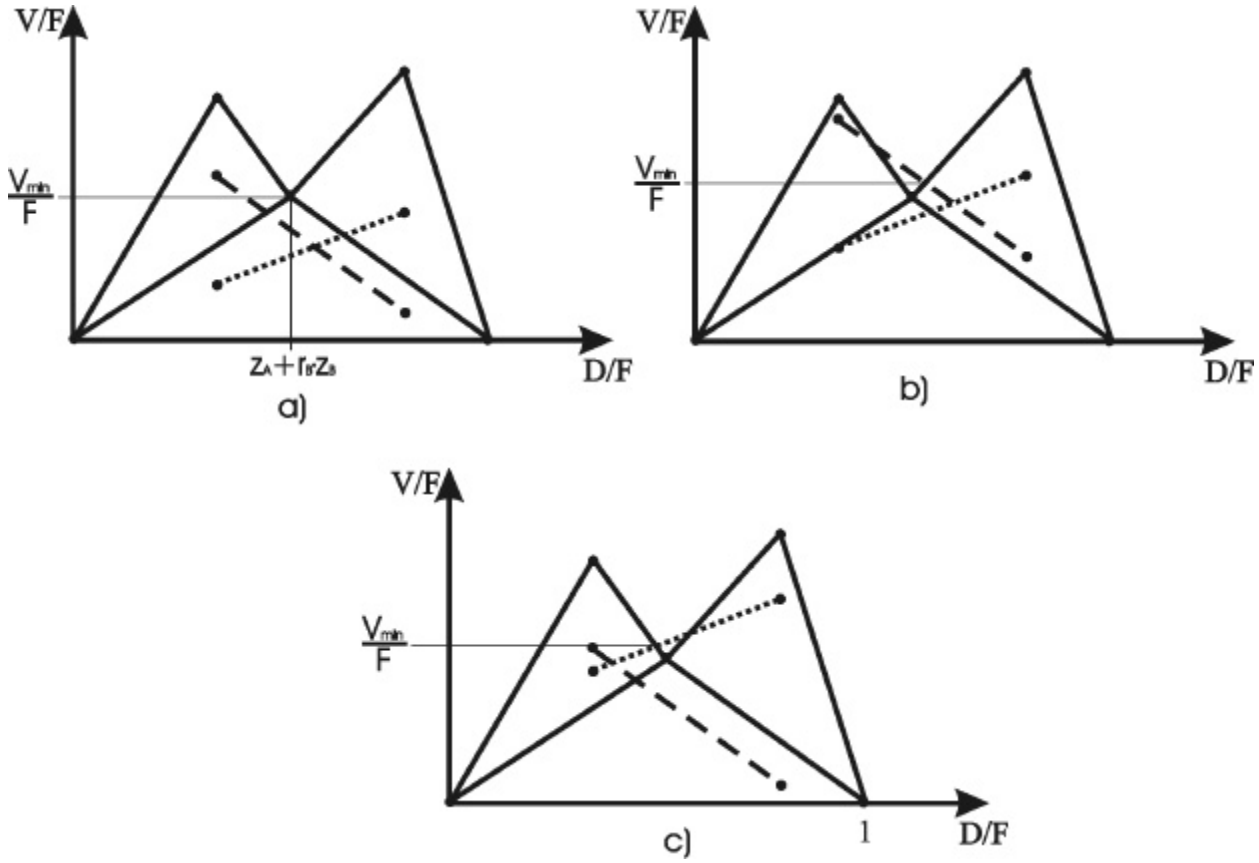

Figure 4.3. Several examples for using diagram for calculation Vmin

When columns are heat integrated, some columns work with more vapour flow rate than they need, for required separation. In Figure 4.3 a) for example columns II and III work with more vapour flow rate, in case b) column I receives a higher vapour flow and in case c) column III receives a higher vapour flow then required.

For real column shown diagrams on Figures above, are not valid. It is now interesting, can we draw some same kind of diagram for real columns. In real columns, we can not make sharp separation, but if composition of a component is lower than some value e, we may say that the separation is sharp. The value of e depends on product purity, for example if the product purity should be 99%, then e is about 1%. Described component is for example heaviest component B in column II (Figure 4.1) were we have "sharp" A/B, or component C in column I where we have "sharp" A/C.

According to simulation results, diagram D/F – Vmin/F for real columns is represented by the dot line in Figure 4.4. The solid line represents minimum flow rate for infinite number of stages. Minimum vapour flow rate for case shown in Figure 4.4 is approximately above minimum flow rate for infinite number of trays, but distillate flow rate for both cases (infinite and finite number of stages) in these case are equivalent. If we increase the number of stages in the second column (columns II and III on Figure 4.1), then the energy consumption will not be decreased, but capital costs will increase. If we increase number of stages in the first column (column I on Figure 4.1), energy consumption will decrease. For low products purity, dotted line can be below the solid line.

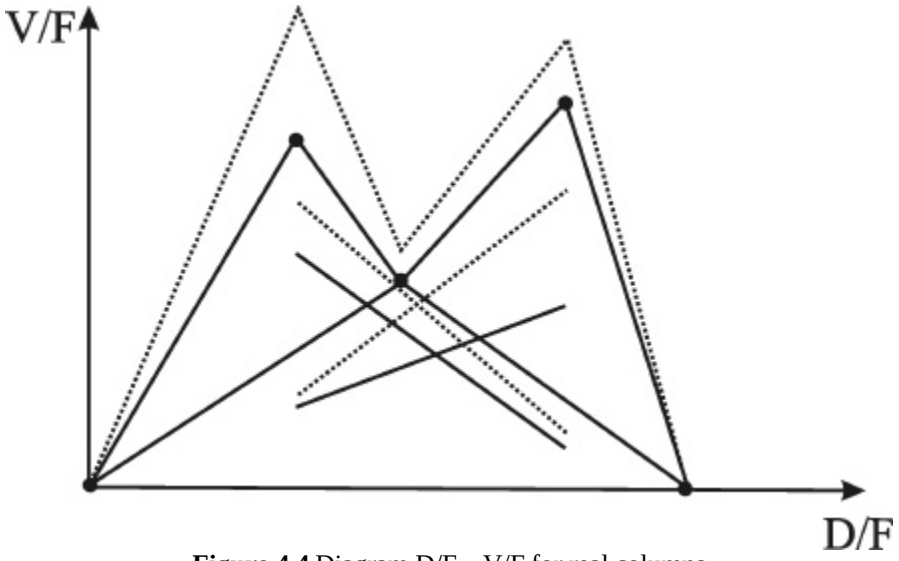

Figure 4.4 Diagram D/F – V/F for real columns

With this knowledge, the diagrams in Figure 4.4 can be used for design of heat-integrated systems.
In Figure 4.5 is represented bad designed system, where second column has fewer trays.

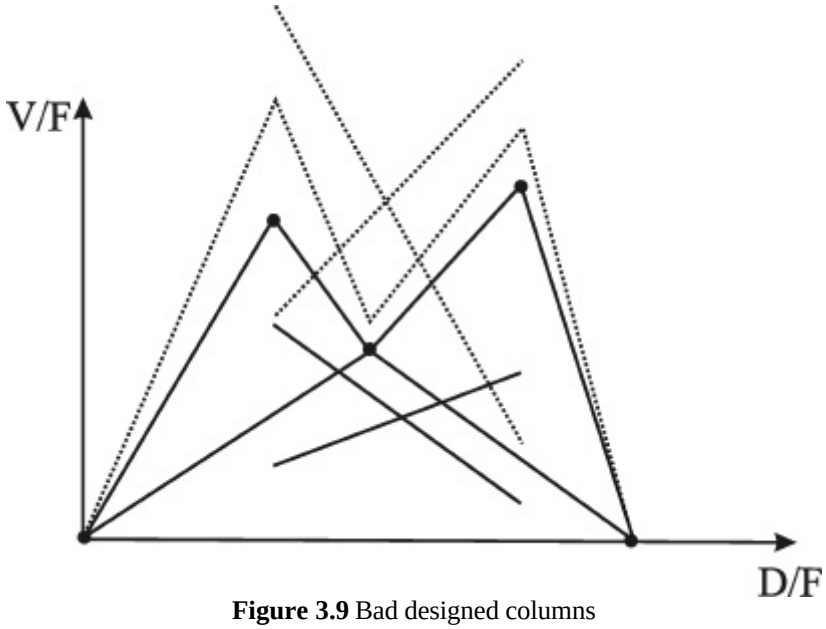

Figure 3.9 Bad designed columns

Whole that the analysis can be done for mixtures with more than three components and systems with more than two columns.

5. Short Cut Calculation

All short cut calculations are based on infinite number of trays, both for the first and second column. In that case, sharp separation can be achieved, which is impossible in real columns.

Using short cut calculations three, ternary mixtures were considered (Table 5.1), these mixtures are taken from literature [12,13, 15,17,18].

\	Mixture 1	Mixture 2	Mixture 3
Component A	**benzene**	**n-pentane**	**Ethanol**
Component B	**Toluene**	**n-hexane**	**n-propanol**
Component C	**m-xylene**	**heptane**	**n-butanol**
Composition	**[0.25; 0.5; 025]**	**[1/3; 1/3; 1/3]**	**[0.4; 0.4; 0.2]**

Table 5.1. Feed data for mixtures

The most promising mixture will be studied further.

Characteristics of the mixtures, such as relative volatility at two different pressure levels, are calculated using a commercial simulation tool ***HYSYS***. Results are shown in Table 5.2, 5.3 and 5.4.

Mixture 1			
/	*a*	ΔH^{sat}	t_m
100 kPa	**[5.57; 2.29; 1.00]**	**46.75 MJ/mol**	**124/139 °C**
600 kPa	**[3.58; 1.88; 1.00]**	**37.44 MJ/mol**	**152/168 °C**

Table 5.2.

Mixture 2			
/	*a*	ΔH^{sat}	t_m
100 kPa	**[7.26; 2.64; 1.00]**	**41.80 MJ/mol**	**84/98 °C**
600 kPa	**[4.50; 2.08; 1.00]**	**32.97 MJ/mol**	**101/120 °C**

Table 5.3.

Mixture 3			
/	*a*	ΔH^{sat}	t_m
100 kPa	**[4.55; 2.22; 1.00]**	**94.2 MJ/mol**	**108/118 °C**
600 kPa	**[3.52; 1.94; 1.00]**	**39.7 MJ/mol**	**131/142 °C**

Table 5.4

The results of short cut calculation are represented in Figures and Tables above.

Mixture 1

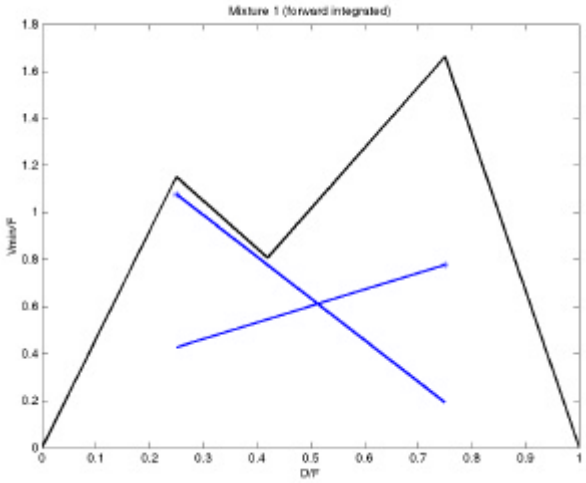

Figure 5.1 Vmin-diagram for ternary feed mixture 1, first column at 6 bar, second column at 1bat pressure.

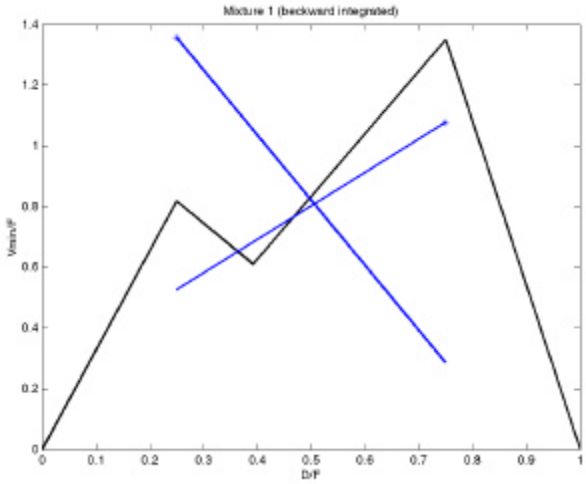

Figure 5.2 Vmin-diagram for ternary feed mixture 1, first column at 1 bar, second column at 6 bar pressure.

Mixture 1			
	not integrated	integrated forward	integrated backward
DS	**1.8972**	**1.1507**	**1.3565**
IS	**2.1270**	**1.6618**	**1.3495**
PF	**1,4400**	**0.807 (D/F=0.4195)**	**0.8274 (D/F=0.4975)**

Table 5.5 Vmin/F for different configurations.

Results in Table 5.5, can be compared with direct split configuration without heat integration. These results are shown in Table 5.6, below.

Mixture 1			
	not integrated	integrated forward	integrated backward
DS	**100%**	**60,7%**	**71,5%**
IS	**112,1 %**	**78,1%**	**71,1%**
PF	**76,6%**	**42,5%**	**43,6%**

Table 5.6 Comparing energy consumption in different configuration based on short cut calculation.

The best possibility for saving energy is configuration with heat-integrated prefractionator (forward integrated).

Mixture 2

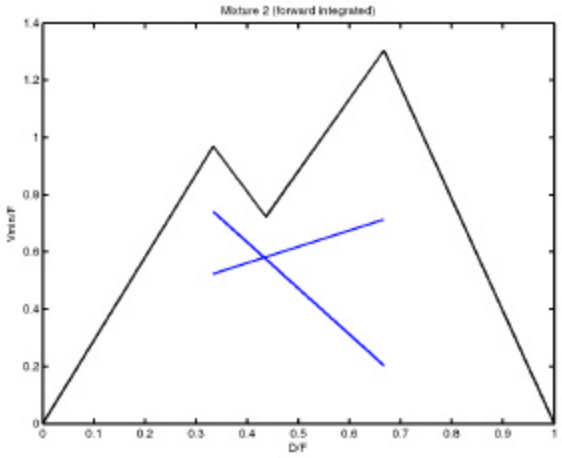

Figure 5.3 Vmin-diagram for ternary feed mixture 2, first column at 6 bar, second column at 1 bar pressure.

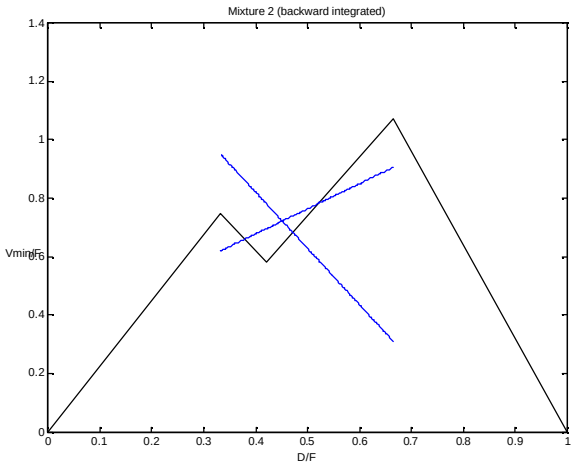

Figure 5.4 Vmin-diagram for ternary feed mixture 2, first column on 1 bar, second column on 6 bar pressure.

Mixture 2			
	not integrated	integrated forward	integrated backward
DS	**1,4881**	**0.9682**	**0.9516**
IS	**1.7840**	**1.3041**	**1.0711**
PF	**1.1800**	**0.7221 (D/F=0.4203)**	**0.7810 (D/F=0.5212)**

Table 5.7 Vmin/F for different configurations.

Results in Table 5.7, can be compared with direct split configuration without heat integration. These results are shown in Table 5.8, below.

Mixture 2			
	Not integrated	integrated forward	integrated backward
DS	**100%**	**65,1%**	**63,9%**
IS	**119,9%**	**87,6%**	**72,0%**
PF	**79,3%**	**48,5%**	**52,5%**

Table 5.8 Comparing energy consumption in different configuration based on short cut calculation.

The best possibility for saving energy is configuration with heat-integrated prefractionator (forward integrated).

Mixture 3

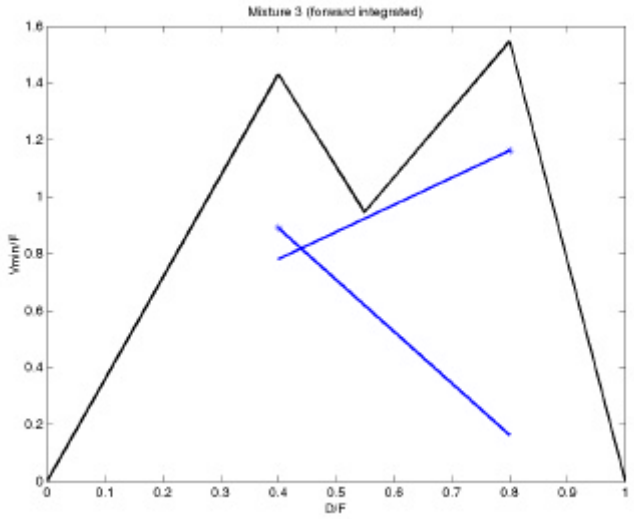

Figure 5.5 Vmin-diagram for ternary feed mixture 3, first column at 6 bar, second column at 1bar pressure.

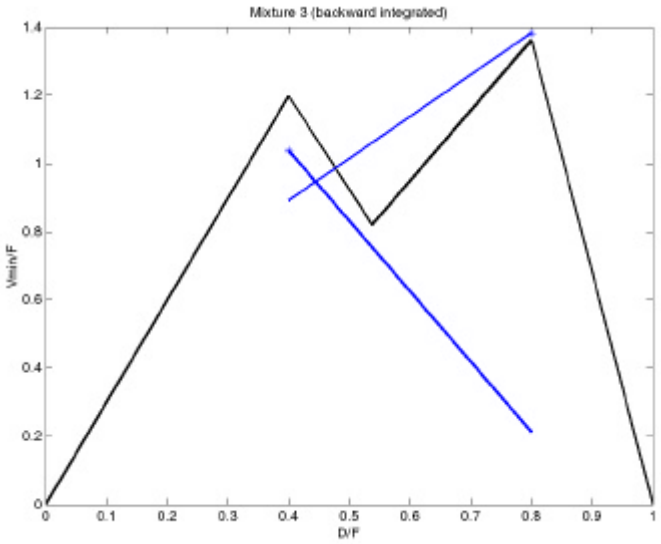

Figure 5.6 Vmin-diagram for ternary feed mixture 3, first column at 1 bar, second column at 6 bar pressure.

Mixture 3			
	not integrated	integrated forward	integrated backward
DS	**2,231**	**1,4304**	**1,1970**
IS	**2,634**	**1.5460**	**1,3823**
PF	**1,7400**	**0,9453 (D/F=0.54897)**	**0.9857 (D/F=0.4770)**

Table 5.9 Vmin/F for different configurations.

Results in Table 5.9, can be compared with direct split configuration without heat integration. These results are shown in Table 5.10, below.

Mixture 3			
	not integrated	integrated forward	integrated backward
DS	**100%**	**64,1%**	**53,7%**
IS	**118,1%**	**69,3%**	**62,0%**
PF	**80,0%**	**42,4%**	**44,2%**

Table 5.10 Comparing energy consumption in different configuration based on short cut calculation.

The best possibility for saving energy is configuration with heat-integrated prefractionator (backward integrated).

6. Finding the Optimum Steady State Solution

In this chapter, with MatLab simulation, optimum working order was calculated for different pressures in the high pressure column and different feed composition. MatLab model is described in Chapter 2.

6.1. Optimum for Different Pressures

For nominal feed composition (0,25 0,5 0,25), constant pressure in the second column, and for various pressure levels in the first column (from 4 bar to 15 bar), optimum (minimum) energy consumption are given in Figure 6.1 below. As it is shown in Figure 6.1 below, with increasing pressure in the first column, energy consumption is decreasing. With increasing pressure in the first column, relative volatility is decreasing, which causes higher energy consumption. However, when increasing the pressure in the first column, heat of vaporization is decreasing, which causes the energy consumption to decrease. Obviously, in the first column, for chosen mixture and pressure level, heat of vaporization has a bigger influence on heat consumption than relative volatility.
In Figure 6.1 temperature difference in the common heat exchanger for the first and second column is also shown. This temperature difference is chosen to be higher or equal to $10\,^{o}C$. For pressure in the first column higher than 5,25 bar the required temperature difference is achieved.
When increasing the pressure in the high-pressure column (first column) the energy consumption is decreasing, but capital costs are increasing, so it is economical to keep the pressure in the first column low. In this work 6 bar was chosen in the first column, and 1,5 bar in second column for further analyses.

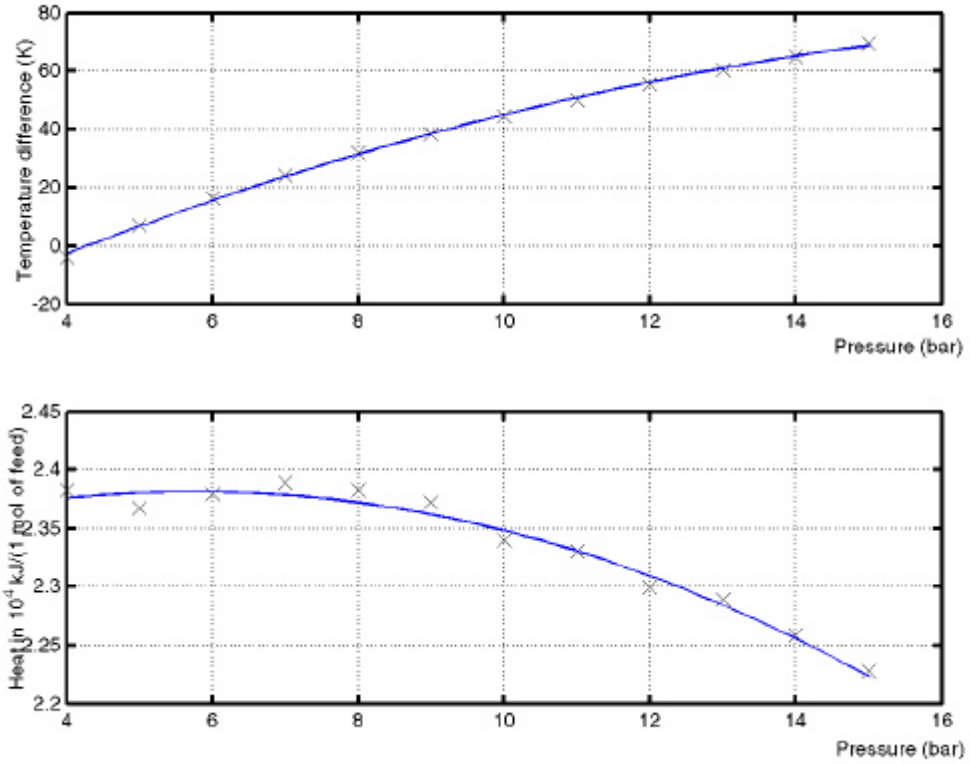

Figure 6.1 Temperature difference and heat consumption for different pressure in first column

6.2. Optimum for Different Feed Compositions

For each feed composition there is different optimum (minimum) consumption of heat energy. Minimum heat consumption in this case is generally function of feed composition, feed flow rate and demand for products purity:

$$Q_{\min} = f\left(Z_f, F, Xp_{\min}\right) \tag{6.1}$$

All other internal variables, e.g. reflux, distillate flow rate, are functions of composition, feed flow rate and demand for products purity in case of minimum energy consumption.

In the considered case the required product purity is 99% and it is constant for calculation. In this model all internal flow rates, in optimum working conditions, are linear function of feed flow rate, so it is not interesting to run simulation for different feed flow rate.
For different feed compositions optimum (i.e. minimum) heat consumption is shown in Table 6.1. Results are calculated using MatLab simulation.

Zfc\Zfa	0,2	0,21	0,22	0,23	0,24	0,25	0,26	0,27	0,28	0,29	0,3
0,2	2,4885	2,4824	2,4729	2,4788	2,4602	2,4888	2,4685	2,4965	2,4996	2,5021	2,504
0,21	2,4663	2,4596	2,4435	2,4496	2,4552	2,4602	2,4646	2,4471	2,4496	2,4768	2,4785
0,22	2,4441	2,4296	2,4368	2,4263	2,4316	2,4363	2,4404	2,4441	2,4471	2,4516	2,4768
0,23	2,4135	2,4071	2,4141	2,3974	2,4029	2,4316	2,4363	2,4404	2,4224	2,4496	2,4496
0,24	2,3916	2,3996	2,3846	2,3913	2,3974	2,3843	2,3885	2,4163	2,4196	2,4471	2,4471
0,25	2,383	2,3696	2,3621	2,3685	2,3743	**2,3796**	2,3843	2,3885	2,4163	2,4196	2,4441
0,26	2,3524	2,3477	2,3552	2,3621	2,3685	2,3743	2,3796	2,3843	2,4124	2,4163	2,4404
0,27	2,331	2,3396	2,3257	2,333	2,3396	2,3457	2,3513	2,3796	2,3843	2,4124	2,4163
0,28	2,3219	2,3096	2,3038	2,3257	2,333	2,3396	2,3457	2,3743	2,3796	2,3885	2,4124
0,29	2,2913	2,2882	2,2963	2,3038	2,3257	2,333	2,3396	2,3457	2,3743	2,3843	2,4079
0,3	2,2813	2,2796	2,2882	2,2963	2,3038	2,3107	2,333	2,3396	2,3513	2,3796	2,3843

Table 6.1 Optimum energy consumption for different feed composition. Unit is 10^4 kJ per 1 mol of feed.

Nominal composition is $Z_f = [0{,}25\ 0{,}50\ 0{,}25]$, and for nominal composition minimum energy consumption is $2{,}3796 \cdot 10^4\ {}^{kJ}/_{1mol\ \ feed}$. Results from Table 6.1, are shown on Picture 6.1.

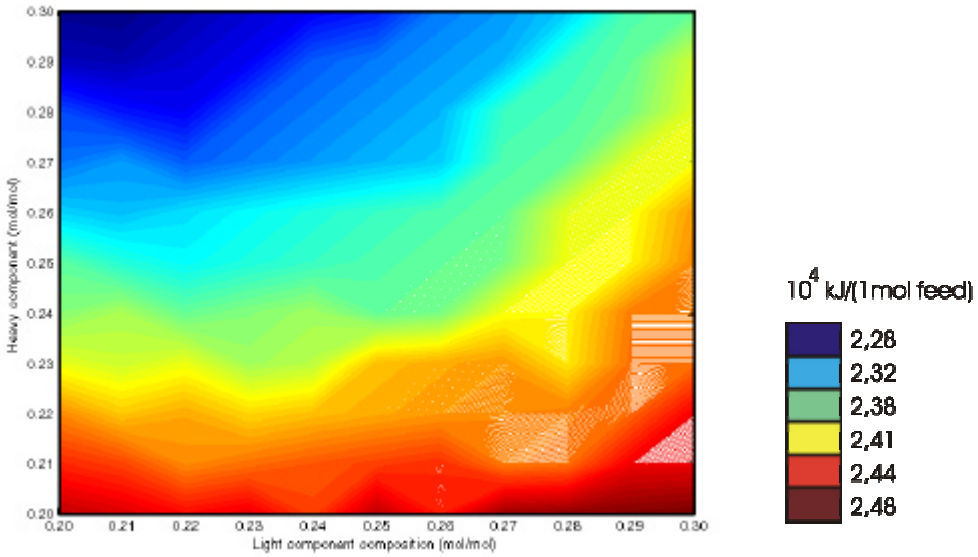

Picture 6.1 Minimum energy consumption for different feed composition

For nominal feed composition **[0,25 0,50 0,25]** and optimal energy consumption compositions of the liquid phase on each tray is shown in Figure 6.2 for the first column and in Figure 6.3 for the second column. Figure 6.4 shows temperature on each tray. Those data are taken from simulations, which is done for system shown in Figure 8.1 in chapter 8, for steady state operation.

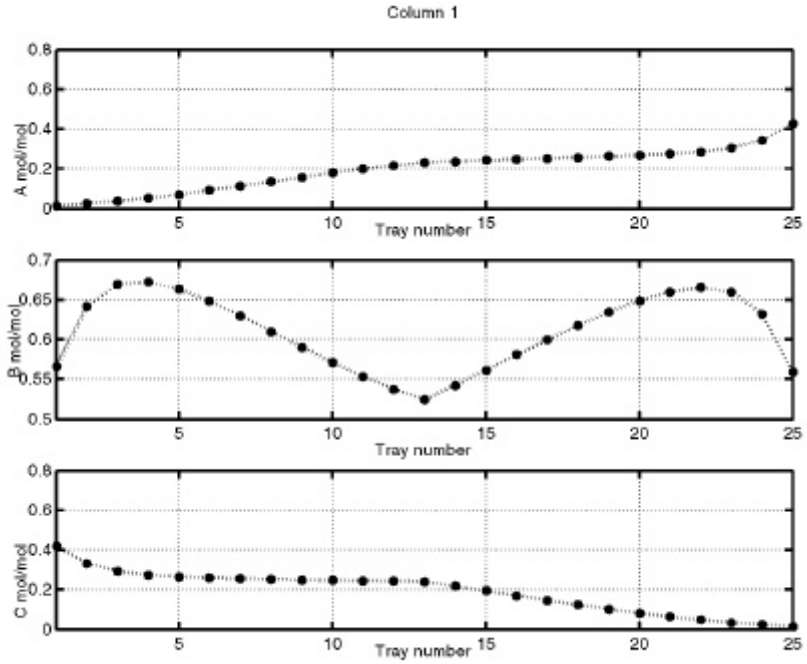

Figure 6.2 Compositions in the first column

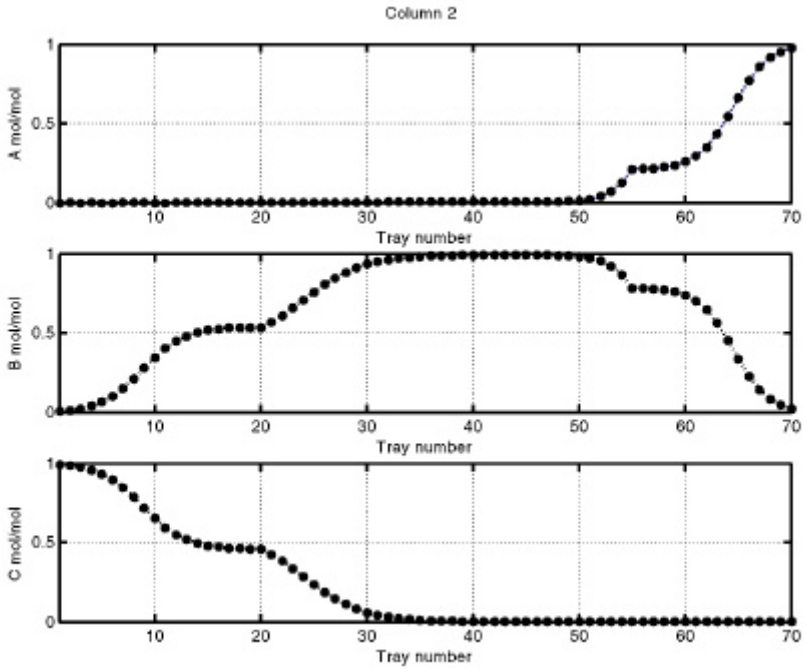

Figure 6.3 Compositions in the second column

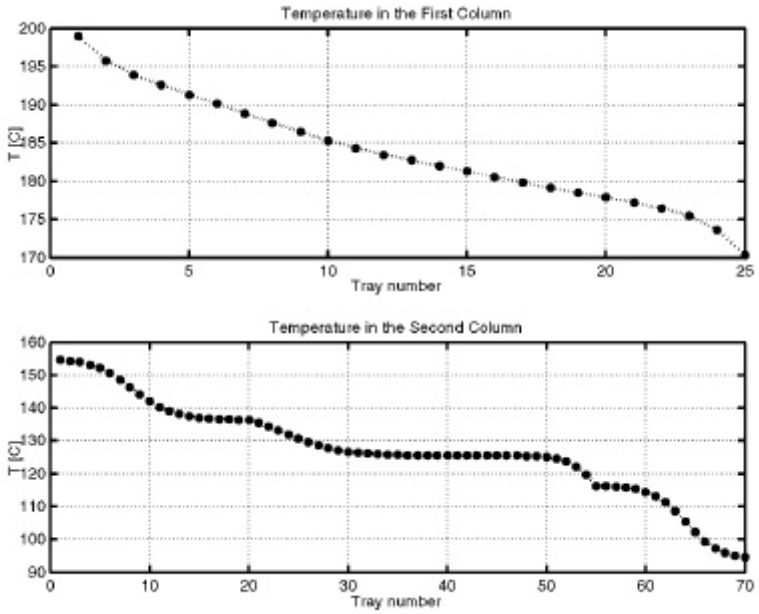

Figure 6.4 Temperature in the first and in the second column

In Figure 6.3 we can see that the second column has more trays then needed. With same energy consumption we can reach product purity with less trays in the second column. In parts between trays number 16 to 20; from 35 to 50 and from 55 to 59 we do not have mass and heat transport, since composition and temperature line on diagrams above is horizontal in this parts. Those trays can be removed, and in system operation, nothing will happen. However, this conclusion is valid only for nominal feed composition. If we have some disturbances in the feed composition or feed flow rate this increased number of trays “may be used”.

7. Simulations Results for Disturbance in Feed Compositions Considering Best Self – Optimisation Value

As is described in Chapter 3 this system has two degrees of freedom (if we assume constant pressures in the first and second column). One independent variable can be used as self-optimisation variable and kept constant. In that case, one independent variable is left for achieving adequate product purity. In this chapter five candidates for self-optimisation are considered:

-flow rate of distillate from the first to the second column,
-temperature of liquid on the bottom in the first column,
-temperature of liquid on the top in the first column,
-composition of light component on the bottom in the first column,
-composition of heavy component in the top in the first column.

Simulations were steady state, without considering trays efficiency and tray behaviour. Changes in the feed flow rate will change optimal variables linearly, so disturbance in the feed flow rate in this case was not studied. Disturbance in feed composition were about 10% of nominal compositions.

Other possible self-optimisation candidates, for example compositions on the bottom in the first columns, temperatures and compositions in the second column, are not considered in this work, but results in that case can be estimated according to results in these simulations.

For each candidate and each simulated disturbances in feed composition, energy consumption is shown in Table 7.1.
Self-optimisation variables are set on optimum value for feed composition [0,25 0,50 0,25], which is nominal composition for feed flow. Because of that, in Table 7.1 for nominal composition heat consumption has to be same as optimal consumption for nominal composition. Differences in these heat consumptions are consequence of numerical accuracy of calculations.

Reflux ratio in the first column is not considered, according to simulation results, changes in reflux have bigger influence on composition in products then changes in flow rate of distillate from first to the second column (this results are not represented in this work).

In tables below all heat consumptions are given in 10^4 kJ/s for 1 mol/sec of feed flow rate (or 10^4 kJ/1 mol of feed).
Q_{rel} is relative heat consumption and it is given as:

$$Q_{rel} = \frac{Q - Q_{opt}}{Q_{opt}} \cdot 100\% \qquad (7.1)$$

Where Q_{opt} is optimum energy consumption for given feed composition. This variable is shown in Table 6.1 in Chapter 6. Relative energy consumption gives increasing heat consumption from optimal energy consumption, and it is good for choosing best self-optimisation variables. For ideal self-optimisation variable relative energy consumption will be zero for all disturbances.

Feed composition [mol/mol]			Optimal energy consumption	Distillate flow rate is constant		Temperature on bottom is constant		Temperature on top is constant		Composition of light component on top is constant	
X_{fA}	**X_{fB}**	**X_{fC}**	**Q_{opt}**	**Q**	**Q_{rel}**	**Q**	**Q_{rel}**	**Q**	**Q_{rel}**	**Q**	**Q_{rel}**
0,2	0,5	0,3	2,3396	2,6086	11,4977	2,6876	14,8743	2,4268	3,7271	2,4854	6,2318
0,21	0,5	0,29	2,2882	2,5614	11,9395	2,634	15,1123	2,4125	5,4322	2,4721	8,0369
0,22	0,5	0,28	2,3038	2,5142	9,1327	2,5703	11,5678	2,4073	4,4926	2,4532	6,4849
0,23	0,5	0,27	2,333	2,467	5,7437	2,5039	7,3253	2,3923	2,5418	2,4421	4,6764
0,24	0,5	0,26	2,3457	2,4434	4,1651	2,4387	3,9647	2,384	1,6328	2,4245	3,3593
0,25	**0,5**	**0,25**	**2,3796**	**2,3961**	**0,6934**	**2,368**	**-0,487**	**2,374**	**-0,235**	**2,4029**	**0,9792**
0,26	0,5	0,24	2,3885	2,4198	1,3104	2,4395	2,1352	2,4685	3,3494	2,3949	0,268
0,27	0,5	0,23	2,4163	2,4906	3,0749	2,5274	4,5979	2,5735	6,5058	2,4996	3,4474
0,28	0,5	0,22	2,4471	2,5614	4,6708	2,6142	6,8285	2,6852	9,7299	2,5976	6,1501
0,29	0,5	0,21	2,4516	2,6558	8,3293	2,7248	11,1437	2,7718	13,0609	2,6971	10,0139
0,3	0,5	0,2	2,4796	2,7266	9,9613	2,8408	14,5669	2,8773	16,0389	2,7881	12,4415
0,2	0,55	0,25	2,383	2,585	8,4767	2,4146	1,3261	2,6044	9,2908	2,6681	11,9639
0,21	0,54	0,25	2,3696	2,5378	7,0982	2,3959	1,1099	2,5454	7,419	2,6138	10,3055
0,22	0,53	0,25	2,3621	2,5142	6,4392	2,388	1,0965	2,5033	5,9777	2,5638	8,539
0,23	0,52	0,25	2,3685	2,467	4,1588	2,383	0,6122	2,4588	3,8125	2,5052	5,7716
0,24	0,51	0,25	2,3513	2,4434	3,917	2,3628	0,4891	2,4071	2,3732	2,4574	4,5124
0,25	**0,5**	**0,25**	**2,3796**	**2,3961**	**0,6934**	**2,368**	**-0,487**	**2,374**	**-0,235**	**2,4029**	**0,9792**
0,26	0,49	0,25	2,3843	2,3961	0,4949	2,3821	-0,092	2,4685	3,5314	2,406	0,9101
0,27	0,48	0,25	2,3885	2,4198	1,3104	2,3961	0,3182	2,5863	8,2813	2,5288	5,874
0,28	0,47	0,25	2,4124	2,467	2,2633	2,4221	0,4021	2,6873	11,3953	2,6349	9,2232
0,29	0,46	0,25	2,4163	2,4906	3,0749	2,4482	1,3202	2,7939	15,6272	2,7354	13,2061
0,3	0,45	0,25	2,4441	2,5378	3,8337	2,484	1,6325	2,8949	18,4444	2,8359	16,0304
0,25	0,55	0,2	2,4646	2,5378	2,9701	3,0087	22,0766	2,5083	1,7731	2,8259	14,6596
0,25	0,54	0,21	2,4404	2,4906	2,057	2,852	16,8661	2,4788	1,5735	2,8523	16,8784
0,25	0,53	0,22	2,4363	2,467	1,2601	2,6906	10,438	2,4494	0,5377	2,8579	17,3049
0,25	0,52	0,23	2,4079	2,4198	0,4942	2,5621	6,4039	2,4201	0,5067	2,483	3,1189
0,25	0,51	0,24	2,3843	2,3961	0,4949	2,4646	3,3679	2,397	0,5327	2,4487	2,701
0,25	**0,5**	**0,25**	**2,3796**	**2,3961**	**0,6934**	**2,3736**	**-0,252**	**2,368**	**-0,487**	**2,4029**	**0,9792**
0,25	0,49	0,26	2,3743	2,3961	0,9182	2,4636	3,7611	2,368	-0,265	2,3686	-0,24
0,25	0,48	0,27	2,3457	2,3961	2,1486	2,5554	8,9398	2,368	0,9507	2,3514	0,243
0,25	0,47	0,28	2,3396	2,3961	2,4149	2,6365	12,6902	2,368	1,2139	2,3456	0,2565
0,25	0,46	0,29	2,333	2,4198	3,7205	2,7253	16,8153	2,3853	2,2417	2,3513	0,7844
0,25	0,45	0,3	2,3107	2,4198	4,7215	2,82	22,0409	2,3796	2,9818	2,3626	2,2461

Table 7.1 Energy consumption for different self-optimisation variables (Q_{rel} [%] ; $Q\left[10^4\ kJ/mol\right]$)

For better understanding, results in Table 7.1 are shown in Figures below. In Figure 7.1 comparison of heat consumptions for first group of disturbance in feed compositions where composition of medium component is constant and equal to 0,5 is shown.
In Figure 7.2 comparison of heat consumptions for second group of disturbance in feed compositions where composition of heavy component is constant and equal to 0,25 is shown.
In Figure 7.3 comparison of heat consumptions for second group of disturbance in feed compositions where composition of light component is constant and equal to 0,25 is shown.

In Figures below (Figure 7.1, Figure 7.2 and Figure 7.3) the solid line is for constant distillate flow rate, the dash line is for constant composition of the light component on the top in first column, the dash-dot is for constant temperature on the top in first column and the dot line is for constant temperature in the bottom in the first column.

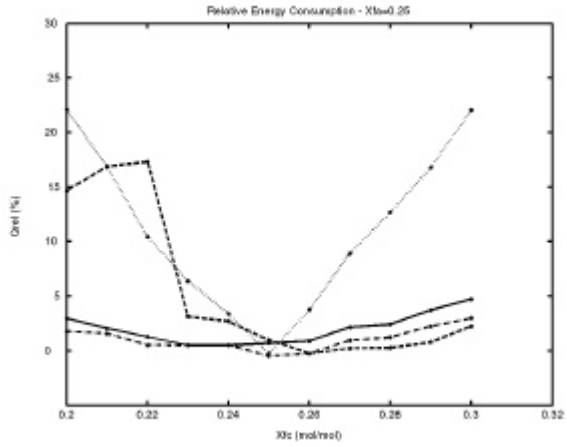

Figure 7.1 Energy consumptions for different self-optimisation variables (composition of the light component in feed is constant)

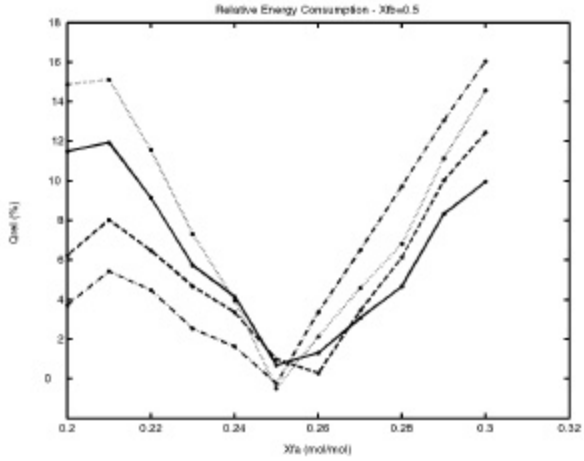

Figure 7.2 Energy consumptions for different self-optimisation variables (composition of the medium component in feed is constant)

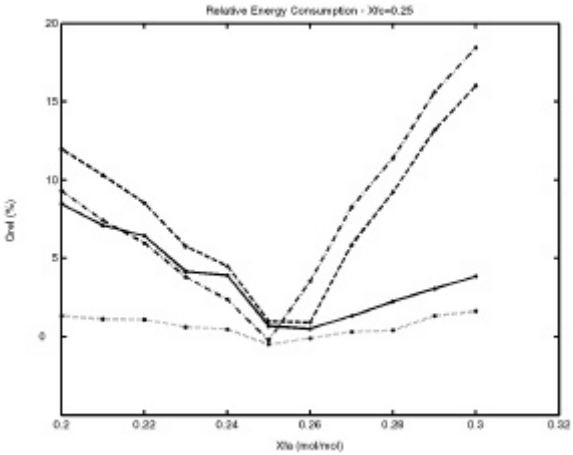

Figure 7.3 Energy consumptions for different self-optimisation variables (composition of the heavy component in feed is constant)

As it is shown in the figures above, there is no best variable for self-optimisation control, for all disturbances. Some variables are good for one type of disturbances, for example increasing the heaviest component composition, but bad for other type of disturbances. For final conclusion from Table 6.1 next disturbances are considered: [0,22 0,5 0,28]; [0,28 0,5 0,22]; [0,25 0,53 0,22]; [0,25 0,47 0,28]; [0,22 0,53, 0,25]; [0,28 0,47 0,25]. For those feed compositions, each candidate increased energy consumptions from optimum are summarized. Results are in Table 7.2 and in Figure 7.4.

\	**[0,22 0,5 0,28]**	**[0,28 0,5 0,22]**	**[0,25 0,53 0,22]**	**[0,25 0,47 0,28]**	**[0,22 0,53 0,25]**	**[0,28 0,47 0,25]**	∑
D=const.	2,5142	2,5614	2,5142	2,467	2,467	2,3961	**0,6186**
Ttop=const	2,5703	2,6142	2,388	2,4221	2,6906	2,6365	**1,0204**
Tbottom=const	2,4073	2,6852	2,5033	2,6873	2,4494	2,368	**0,7992**
Xa top=const	2,4532	2,5976	2,5638	2,6349	2,8579	2,3456	**1,1517**

Table 7.2 Summarized heat consumptions for different self-optimisation variables

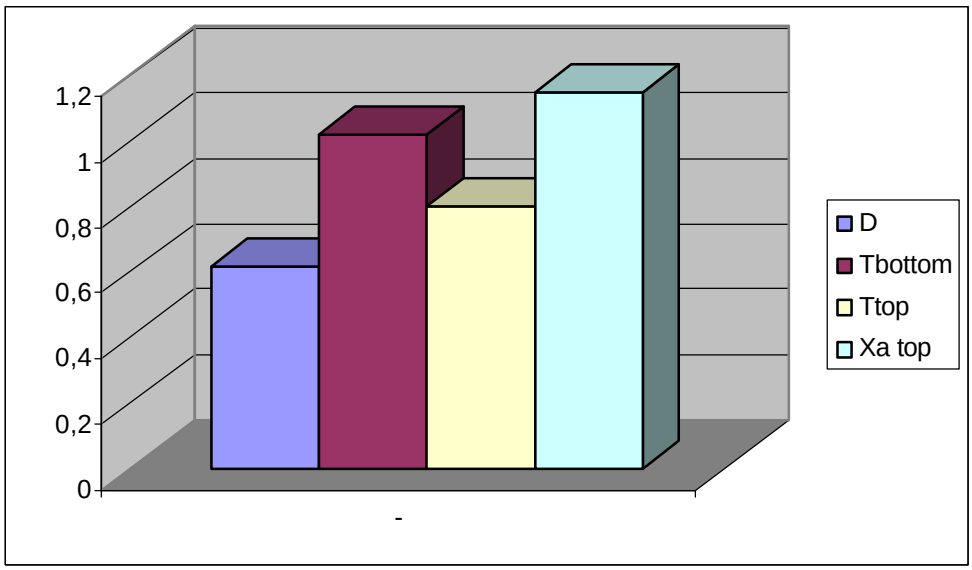

Figure 7.4. Results from Table 6.2, summarized heat consumptions for different self-optimisation variables

The best variable for self-optimisation control, according to results shown in Figure 7.4 above is distillate flow rate in the first column. The worst self-optimisation variable is composition of light component on top of first column.

Composition of heavy component on the top in first column was also considered. These results are shown in Table 7.3, below. Unfortunately, accuracy was not high enough, so results are scattered. Results from Table 7.3, are compared with results for constant distillate flow rate. Comparisons are showed in Figures 7.4, 7.5 and 7.6.

Feed composition			Optimal energy consumption	Composition of heavy component on top is constant	
X_{fA}	X_{fB}	X_{fC}	Q_{opt}	Q	Q_{rel}
0,2	0,5	0,3	2,3396	2,3096	-0,01282
0,21	0,5	0,29	2,2882	2,2902	0,000874
0,22	0,5	0,28	2,3038	2,3455	0,018101
0,23	0,5	0,27	2,333	2,3631	0,012902
0,24	0,5	0,26	2,3457	2,3784	0,01394
0,25	**0,5**	**0,25**	**2,3796**	**2,3973**	**0,007438**
0,26	0,5	0,24	2,3885	2,4173	0,012058
0,27	0,5	0,23	2,4163	2,4352	0,007822
0,28	0,5	0,22	2,4471	2,4518	0,001921
0,29	0,5	0,21	2,4516	2,4695	0,007301
0,3	0,5	0,2	2,4796	2,4855	0,002379
0,2	0,55	0,25	2,383	2,3777	-0,00222
0,21	0,54	0,25	2,3696	2,3788	0,003883
0,22	0,53	0,25	2,3621	2,3871	0,010584
0,23	0,52	0,25	2,3685	2,3893	0,008782
0,24	0,51	0,25	2,3513	2,3937	0,018033
0,25	**0,5**	**0,25**	**2,3796**	**2,3973**	**0,007438**
0,26	0,49	0,25	2,3843	2,4031	0,007885
0,27	0,48	0,25	2,3885	2,4112	0,009504
0,28	0,47	0,25	2,4124	2,4159	0,001451
0,29	0,46	0,25	2,4163	2,4228	0,00269
0,3	0,45	0,25	2,4441	2,4318	-0,00503
0,25	0,55	0,2	2,4646	2,5786	0,058022
0,25	0,54	0,21	2,4404	2,5014	0,005286
0,25	0,53	0,22	2,4363	2,4247	-0,00213
0,25	0,52	0,23	2,4079	2,4203	0,005067
0,25	0,51	0,24	2,3843	2,4118	0,010317
0,25	**0,5**	**0,25**	**2,3796**	**2,3973**	**0,007438**
0,25	0,49	0,26	2,3743	2,3853	0,002232
0,25	0,48	0,27	2,3457	2,3731	0,009294
0,25	0,47	0,28	2,3396	2,3604	0,00889
0,25	0,46	0,29	2,333	2,3477	0,006301
0,25	0,45	0,3	2,3107	2,3318	0,007833

Table 7.3 Energy consumption for heavy component on the top in first column as self-optimisation variable

$$(Q_{rel}\,[\%]\,;\,Q\left[10^4\,{}^{kJ}\!/_{mol}\right])$$

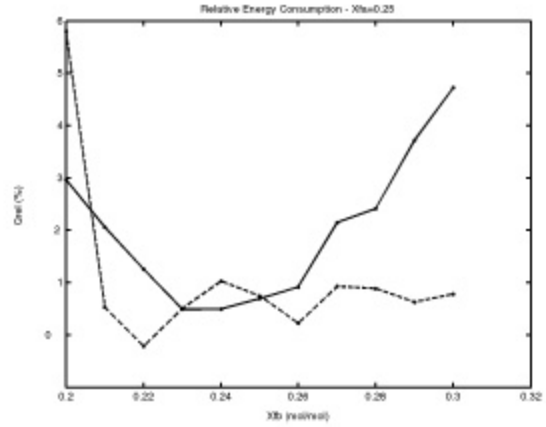

Figure 7.4 Energy consumptions for different self-optimisation variables (composition of light component in feed is constant)

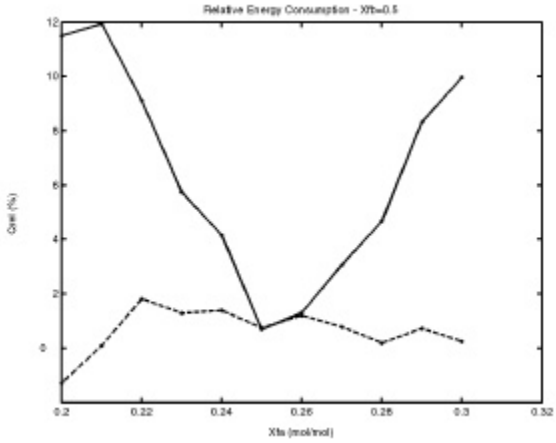

Figure 7.5 Energy consumptions for different self-optimisation variables (composition of medium component in feed is constant)

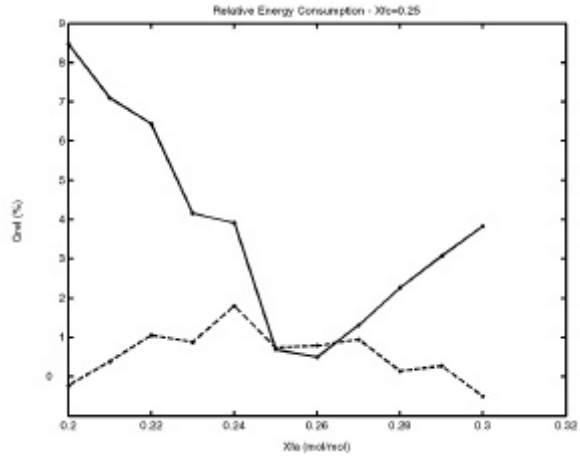

Figure 7.6 Energy consumptions for different self-optimisation variables (composition of heavy component in feed is constant)

In Figures above, solid line is for constant distillate flow rate between columns, and dash line is for constant composition on the top in the first column.

Figure 7.7 is the same figure as Figure 7.4 but only for constant distillate flow rate and for constant heavy component on the top in first column. As it is shown on the Figure 7.7 below, the best self-optimisation variable is heavy component composition on the top in the first column. Since this composition is very low, in first column separation is close to sharp separation, due to high purity of final products.

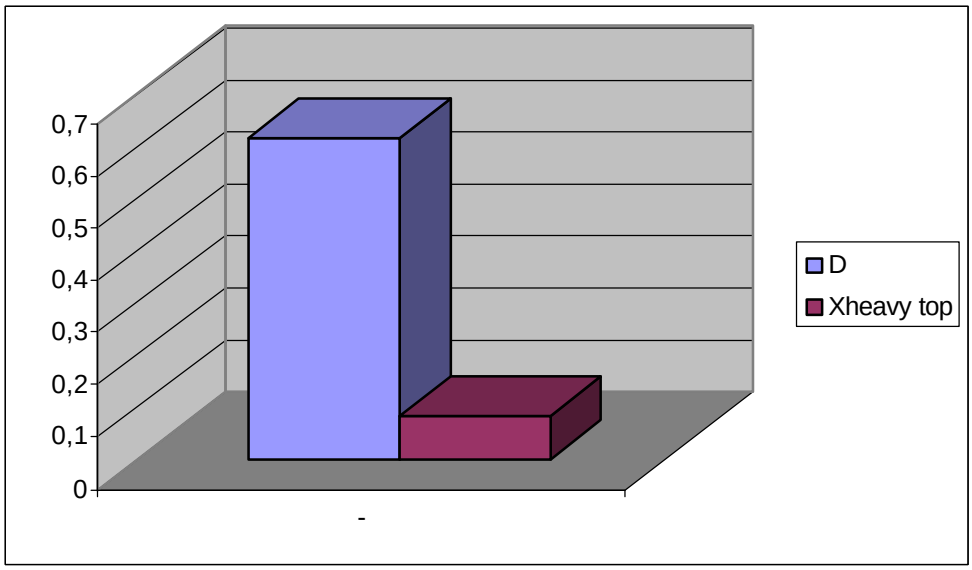

Figure 7.7 Summarized heat consumptions for self-optimisation variables
(constant distillate flow rate and constant heavy component composition on the top in first column)

As represented on Figure 7.7 and 7.4 the best self-optimisation variable is the composition of the heaviest component on the top in the first column. If this variable is kept constant, according to Figure 7.4, 7.5 and 7.5, then the increase of heat consumption will be low compared to the optimal consumption. From simulation results, composition of heaviest component on the top in first column should be ***0.0144 mol/mol*** on the top tray. In Chapter 4 is describes "sharp" separation in real columns, and we can conclude that the first column should work as "sharp" AB/BC. With keeping top composition of heaviest component in the first column enough low, we have "sharp" AB/BC, and we are close to optimum performance of distillation system. This conclusion is used in next chapter, where dynamical behaviour of system is considered.

8. Simulation of Dynamical Performance of System with Prefractionator

As is described in Chapter 7, the best self-optimisation variable for the system considered is composition of the heaviest component on the top in the first column. This composition, according results from simulations, should be ***0,0144 mol/mol*** on the top tray**.** If we keep this composition constant, we are very close to optimal energy consumption (Figure 7.4, Figure 7.5 and Figure 7.6). When keeping constant composition of heaviest component, the first column (prefractionator) works as “sharp” AB/BC. Figure 8.1 shows haw one possible solutions, for the implementation of a control scheme, based on the above results. The control scheme presented in Figure 8.1 has been used for the dynamic simulations.

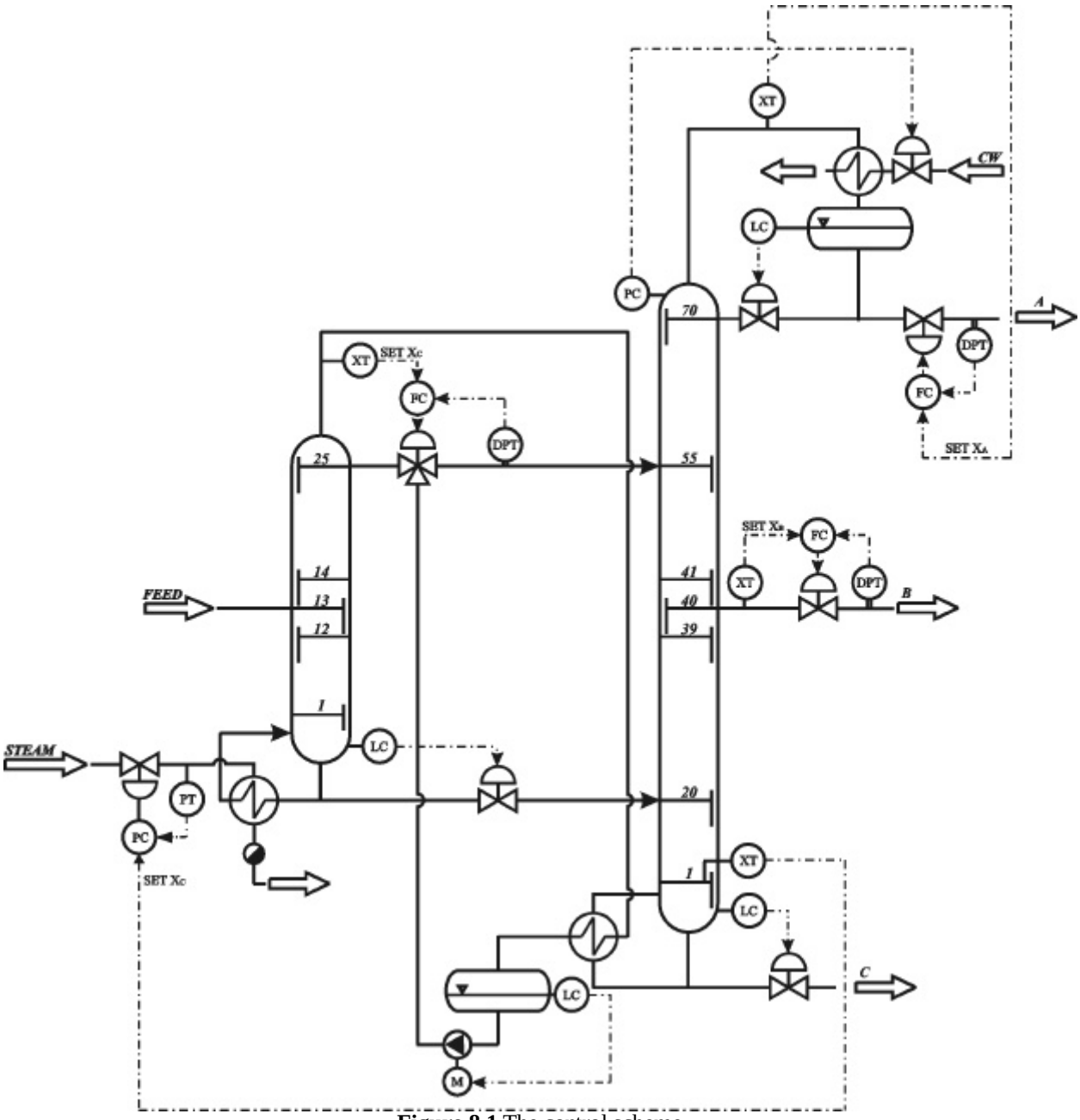

Figure 8.1 The control scheme

Composition of the product C is controlled with the vapour flow rate control valve in the bottom of first column. Composition of product B is controlled, using control of flow rate of side stream. Composition of product A is controlled changing reflux in the second column. Composition of heaviest component in the distillate from the first column is also controlled using reflux. This control loop is chosen according results from self-optimisation study. The most difficult control loop in this system is the connection between composition of the bottom product and evaporator duty for the first column. This is because of the inertia of the system and it is very important in case of periodic disturbances. Evaporator duty for first column is controlled using pressure control valve for steam supply

The simulation model is simplified. It is assumed that all level controls work perfect. Pressure control in first column was assumed perfect. Simplified model, simulated in this work is shown on Figure 8.2.

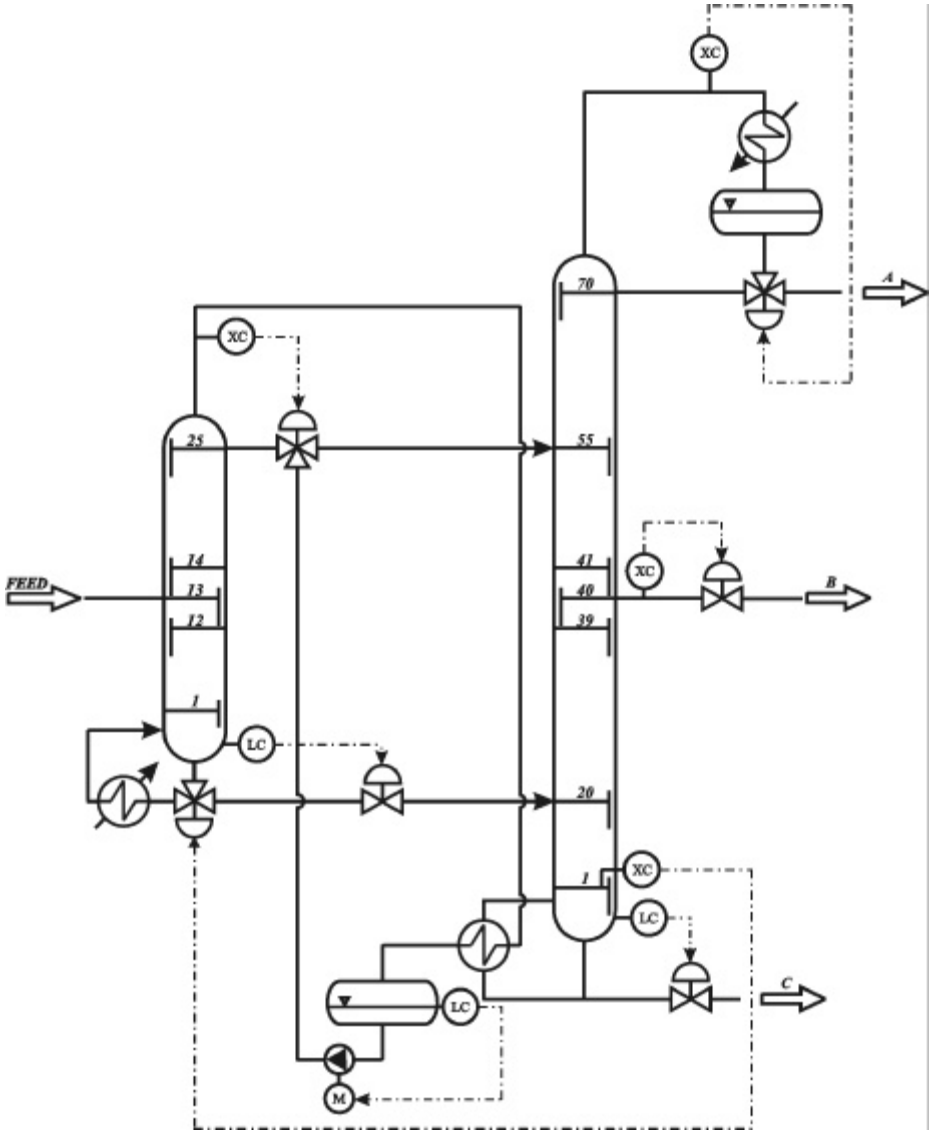

Figure 8.2 Simplified model

Nominal feed composition in the simulation was [0.25 0.50 0.25] and nominal feed flow rate was 0.1 mol/s. Simulation was done for two disturbances in composition: [0.28 0.44 0.28] and [0.22 0.56 0.22] and for two disturbances in feed flow rate 0.9 and 0.11 m/s. All disturbances

happened 100 second after starting moment. Before disturbances, performance was steady for nominal composition and nominal feed flow rate. On Figure 8.3 and Figure 8.4, below is given result for disturbances in feed composition.

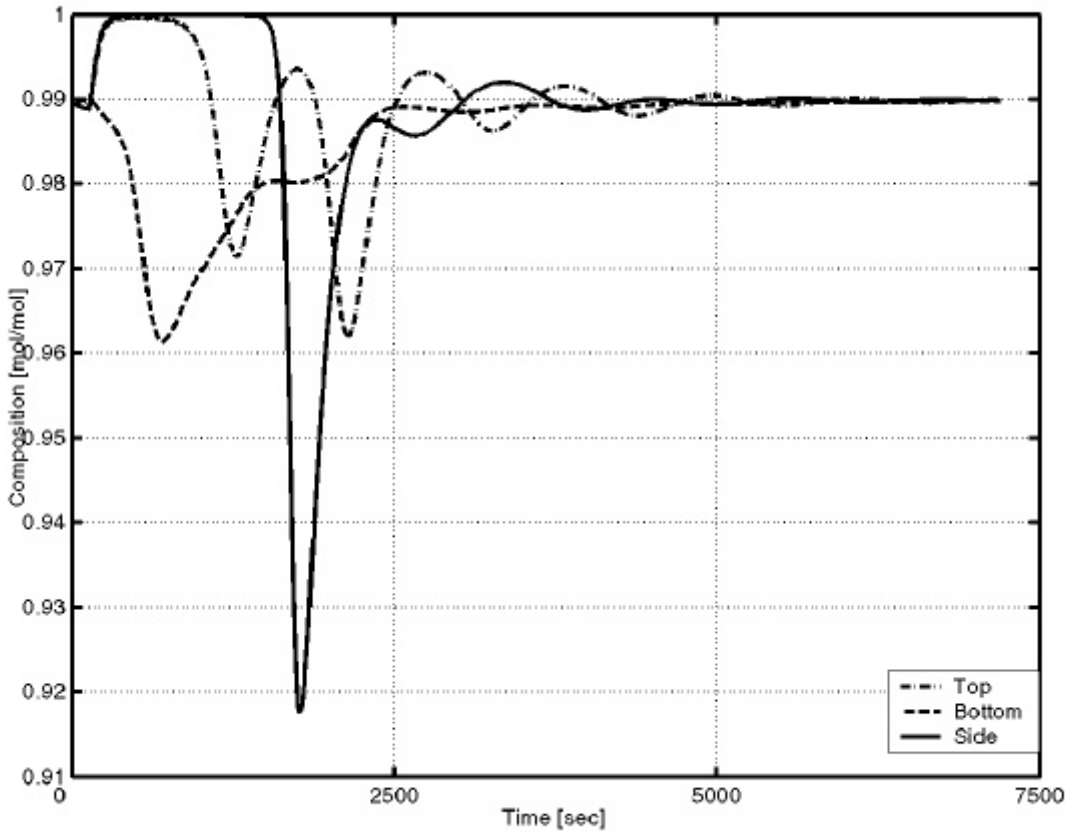

Figure 8.3 Product composition. Disturbance in feed composition [0.28 0.44 0.28]

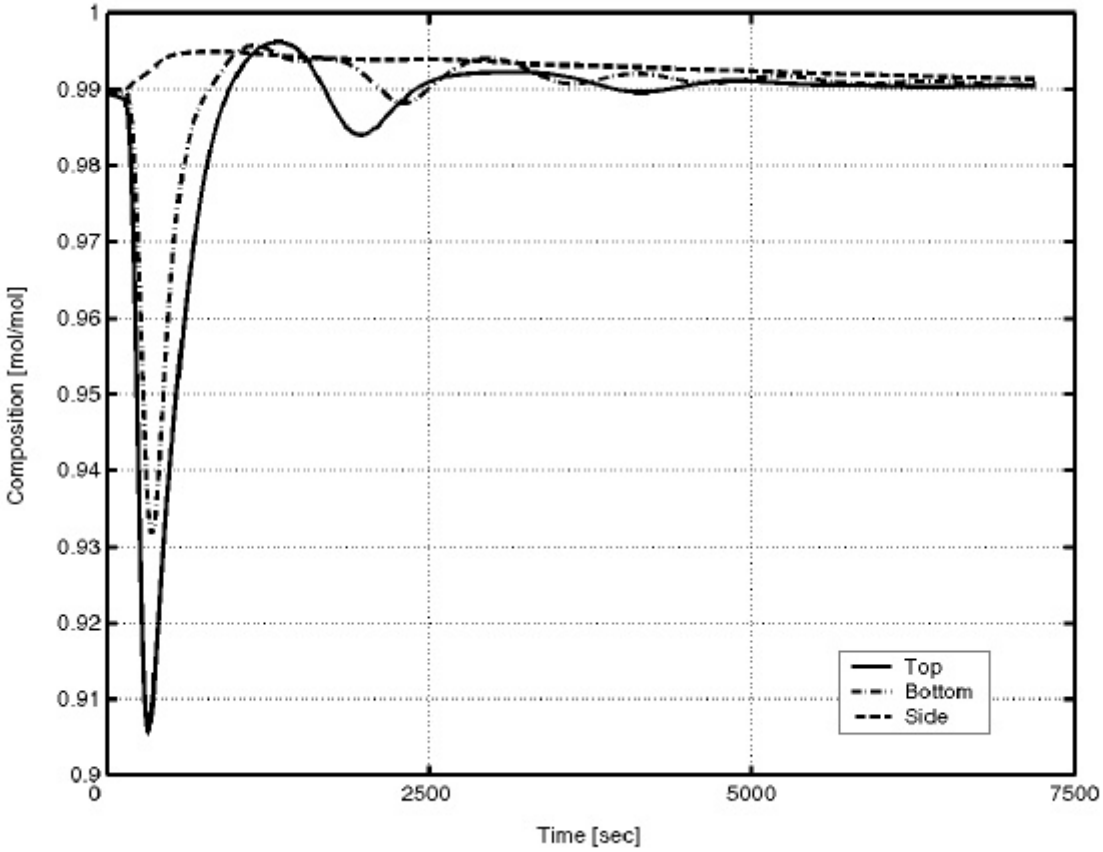

Figure 8.4 Product composition. Disturbance in feed composition is [0.22 0.56 0.22]

According to results shown on figures above, after about 300 second, we have composition of final product higher than 98%, which is acceptable, for disturbances [0.22 0.56 0.22], and after 2300 second for disturbance [0.28 0.44 0.28].
In simulation PI controllers were used. Proportional gain was twice higher for compositions above 0.995.

Result for disturbances in feed flow rates are shown in Figure 8.5 and Figure 8.6, on the next page.

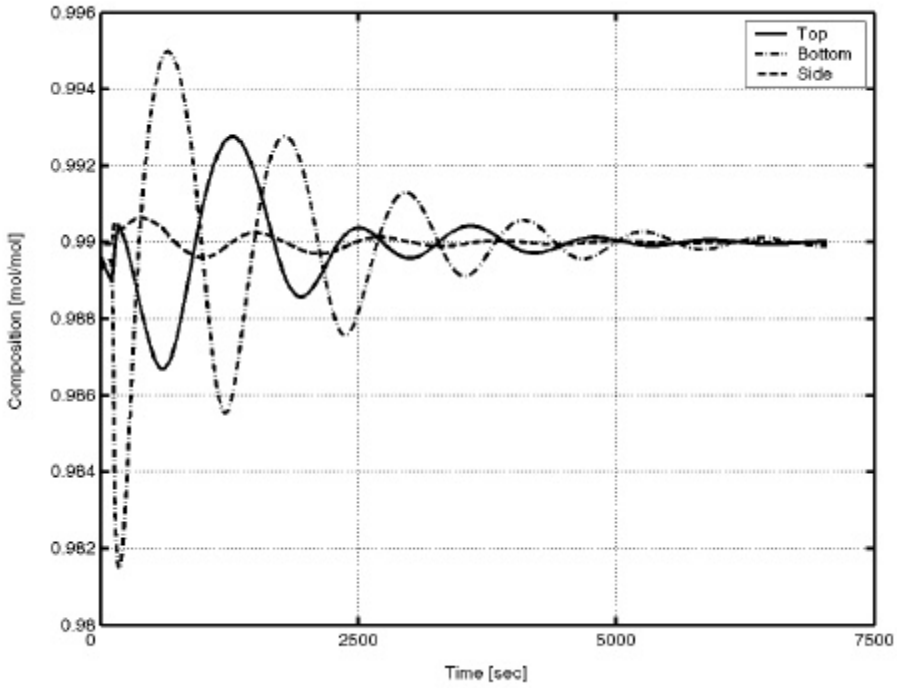

Figure 8.5 Product composition. Disturbance in feed flow rate, 0.9 mol/s

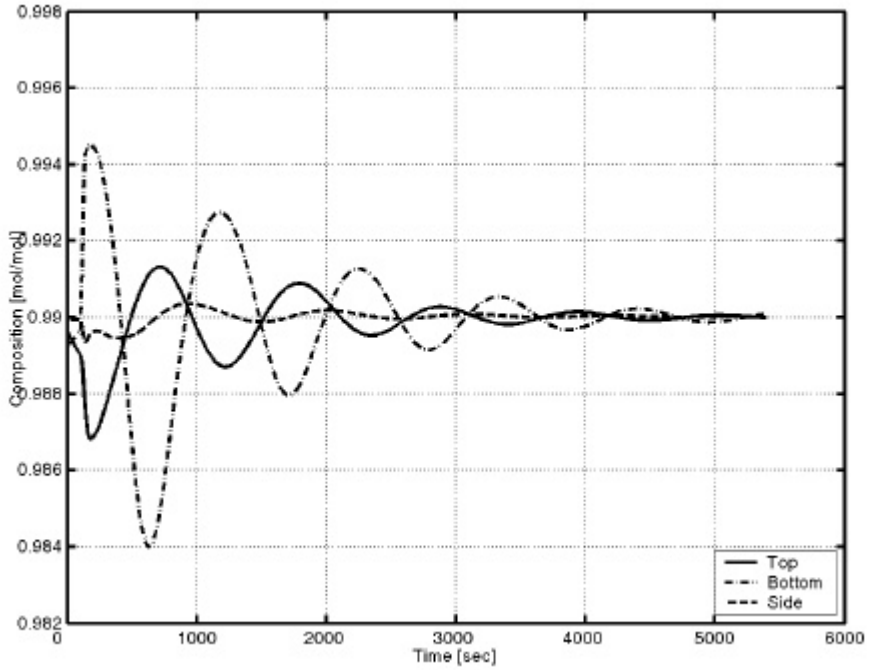

Figure 8.6 Product composition. Disturbance in feed flow rate, 0.11 mol/s

According results in Figures above, disturbances in feed flow rate do not have big influence on products composition.

According to simulation results, we may conclude that it is possible to control this system and keep product composition at 99%. Disturbances in feed flow rate, as is shown on Figure 8.5 and Figure 8.6 do not make big disturbances in products composition. In simulated cases, feed disturbances did not make bigger changes in products compositions than $\begin{matrix}+0,05\% \\ -0,91\%\end{matrix}$. Disturbances in feed compositions, as is shown on Figure 8.3 and Figure 8.4, made big changes in product composition, but only temporally. A biggest disturbance in product composition in that case was $\begin{matrix}+1,01\% \\ -8,59\%\end{matrix}$.

In Figure 8.7 results for simulation in which the set point for composition of products are changed from 90% on 99% are shown. Before changing the set points the system was working at steady with composition of products at 90%.

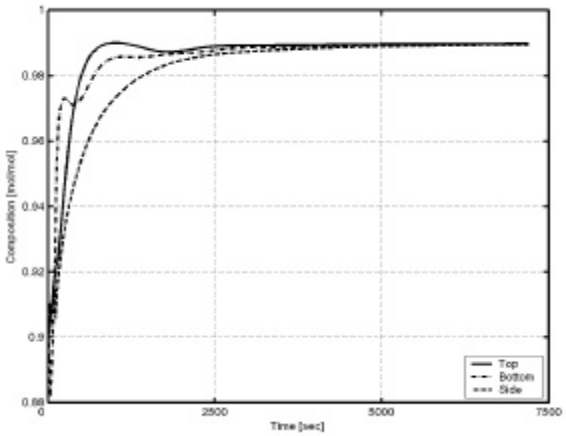

Figure 8.7 Changing set compositions in products

As it is shown in the Figure, steady working order is reached after approximately 2500 seconds. In Figure 8.8 below results of simulation with periodical disturbances is shown. Composition of the heaviest and light component in feed flow rate was changed as sinus function between 0.22 and 0.28 mol/mol every 1600 seconds. Same simulation, but for slower changes in feed composition (every 3600 seconds), was done and results are shown in Figure 8.9.

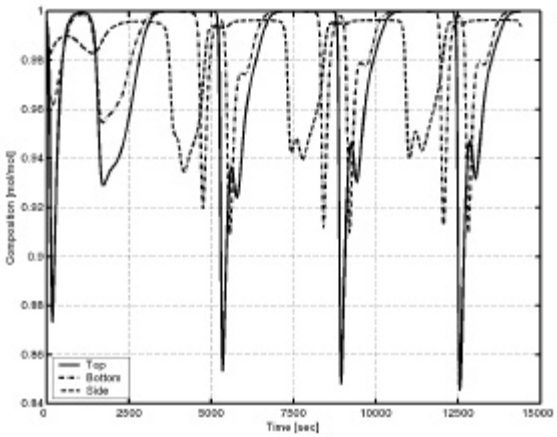

Figure 8.8 Periodical changes in feed composition

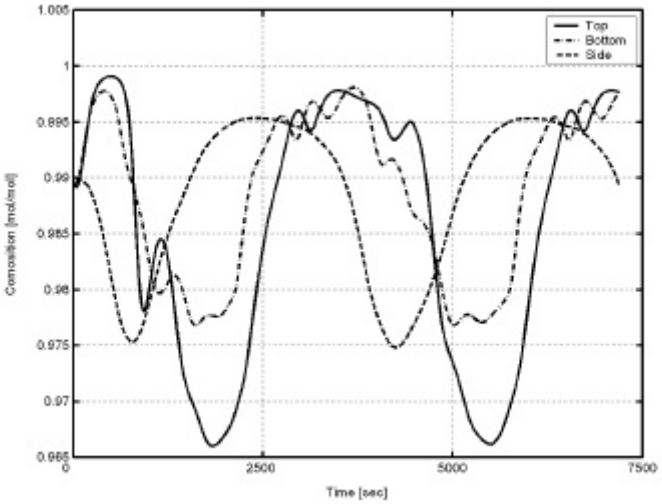

Figure 8.9 Slower periodic changes in feed composition

Basic problem with the control of this system is the demand for high products purity. Figure 8.10 shows the same simulation but for 90% product composition. The disturbance was [0.28 0.44 0.28] (nominal feed composition, before disturbance was [0.25 0.50 0.25]). As is shown on Figure 8.10 this system with lower purity products is much easier to control.

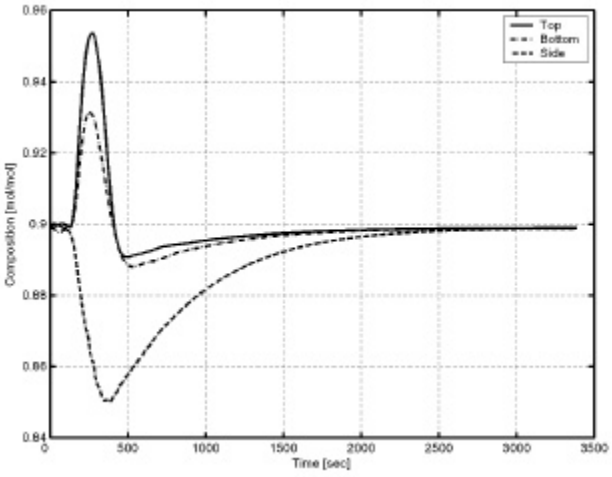

Figure 8.10 Product purity is 90%

Same periodic disturbances as for products purity of 99% was done but for product purity of 90%. Results are shown on Figure 8.11.

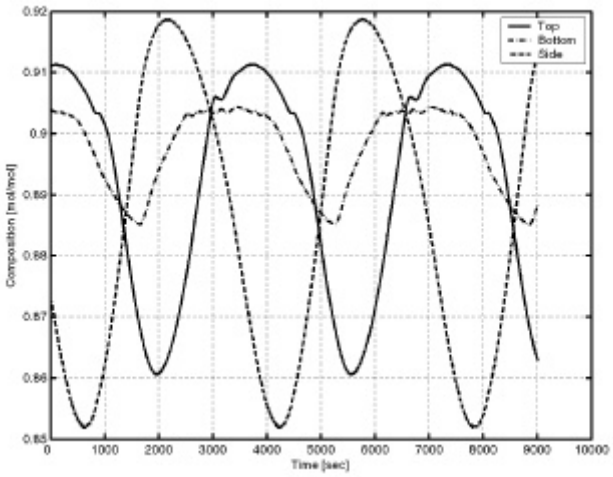

Figure 8.11 Periodic disturbances. Set point for product purity is 90%

Sudden changes in feed composition and feed flow rate in practise are not common. Usually changes are continuous. In Figure 8.12, one continues change in feed composition is simulated. From nominal composition to composition [0.28 0.44 0.28] is changed for 3000 seconds. As is shown in the Figure, purity of products are higher than 98%.

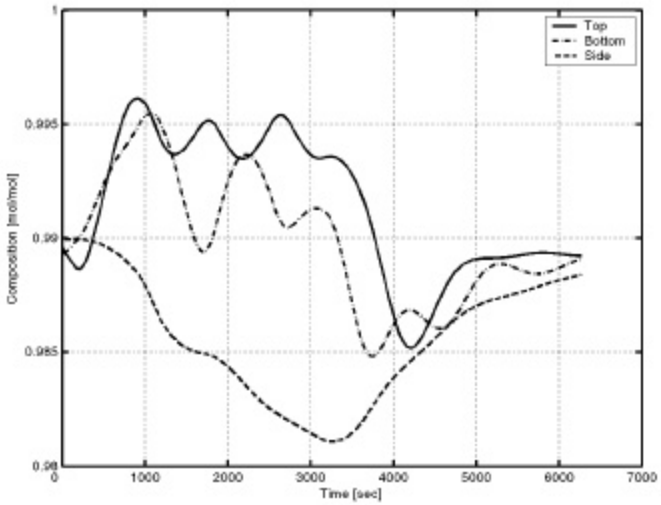

Figure 8.12 Continues changes in feed composition

9. Conclusions

In this work, possibilities for saving energy using heat-integrated system with prefractionator in ternary mixture separations were considered. According to analysis results of short cut calculations, this system can save more than 60% energy compared with the conventional direct split system without heat-integration.

For choosing a good control solution self-optimisation analyse was done. The best self-optimisation variable was found to be the composition of the heaviest component at the top in first column. It wasn't simulated, but we can conclude that same results will be if self-optimisation variable is composition of heaviest component on the bottom in the first column.

Dynamical simulations were also considered. For lower product purity, control is much easier, but not for high purity of products. For better and stabile control, composition transmitter for control of top product in the first and second column is on the vapour side before the vessels. Transmitter for control of bottom composition in the second column measure composition on the first tray, also before the vessel. With these solutions, control is stabilised. According to simulation results, this system can be controlled. Solution on Figure 8.1 gives good results. With better tuning, results can be even better. As is shown in Figure 8.11, for slower disturbances in feed flow, control of the system is very good. To avoid sudden changes in feed composition and feed flow rate good solution could be to use feed tank, or products tanks.

Further investigation could be find other control solutions with better control performance. There are also possibilities for implementing this system for separation of mixtures with more components than three. It can be a system with high energy saving, but according to these simulations very difficult for control.

References

1. King, C. J., “Separation Processes”, McGraw-Hill Inc., New York, 1980.
2. Shinskey, F. G., “Distillation Control”, McGraw-Hill Inc., Massachusetts, 1984.
3. Buckley, P. S., Luyben, W. L., Shunta, J. P., “Design of Distillation Column Control”, Instrument Society of America, 1985.
4. Nocedal, J., Wright, S. J., “Numerical Optimisation”, Springer – Ver log, New York, 1999.
5. Luyben, W. L. “Process Modelling, Simulation, and Control for Chemical Engineers”, McGraw-Hill Inc., New York, 1973.
6. Franks, G. E. R. “Modelling and Simulation in Chemical Engineering”, Wiley, Canada, 1972.
7. Conte, S. D., Boor, C. “Elementary Numerical Analysis”, McGraw-Hill Inc., USA, 1998.
8. Kister, H. Z., ”Distillation Operation” McGraw-Hill Inc., New York, 1990.
9. Balchen, J. G., Mumme, K. I., Reinhold, N., ”Process Control”, McGraw-Hill Inc., New York, 1988.
10. Larsson, T., Skogestad, S., ”Control of an Industrial Heat Integrated Distillation Column”, Presented at the AIChE annual meeting, Dallas, 1999.
11. Collura, M. A., Luyben, W. L., ”Energy-Savings Distillation Designs in Ethanol Production”, Ind. Eng. Chem. Res., 27, p1686-1696, 1988.
12. Agrawal, R., Fidkowski, T., Xu, J., “Prefractionation to Reduce Energy Consumption in Distillation without Changing Utility Temperatures”, Aiche Journal, Separations, p2118-2127,1996.
13. Chaing, T., Luyben, W. L., “Comparison of Energy Consumption in Five Heat-Integrated Distillation Configurations”, Ind. Eng. Chem. Des. Dev., 22, p175-179,1983.
14. Tyreus, B. D., Luyben, W. L., “Two towers cheaper then one?”, Hydrocarbon Processing, p 93-96, July,1975.
15. O’Brien, N. G., “Reducing Column Steam Consumption”, CEP, p65-67, July, 1976.
16. Skogestad, S., “Dynamics and Control of Distillation Columns: A Tutorial Introduction”, Trans IChemE, Vol 75, Part A, September, 1997.
17. Annakou, O., Mizsey, P., “Rigorous Comparative Study of Energy-Integration Distillation Schemes”, Ind. Eng. Chem. Res., 35, p1877-1885, 1996.
18. Wankat, P. C., ”Multieffect Distillation Processes”, Ind. Eng. Res., 32, p894-905, 1993.
19. Skogestad, S., Morari, M., ”Understanding the Dynamics Behavior of Distillation Columns”, Ind. Eng. Chem. Res., 27, p 1848-1862,1988.
20. Ding, S. S., Luyben, W. L., “Control of a Heat-Integrated Complex Distillation Configuration”, Ind. Eng. Chem. Res., 29, p 1240-1249, 1990.
21. Halvorsen, I. J., ”Minimum Energy Requirements in Complex Distillation Arrangements”, PhD Thesis, Norwegian University of Science and Technology, Trondheim, Norway, 2001.
22. Engelien, H. K., ”Process Integration Applies to the Design and Operation of Distillation Columns”, PhD Thesis, Norwegian University of Science and Technology, Trondheim, Norway, 2004.
23. Jacimovic, B., Genic, S., “Toplotne operacije i aparati”, Masinski fakultet, Beograd, 1992.